2046 Molecular Testing in Anatomic Pathology and Adherence To Guidelines: A College of American Pathologists Q-PROBESTM Study of 2230 Testing Events Reported By 26 Institutions

Keith Volmar, Michael Idowu, Rhona Souers, Raouf Nakhleh. Rex Healthcare, Raleigh, NC; Virginia Commonwealth University Health System, Richmond, VA; College of American Pathologists, Northfield, IL; Mayo Clinic Florida, Jacksonville, FL.

Background: Appropriate and timely performance of molecular testing in anatomic pathology is an indicator of quality. The National Comprehensive Cancer Care Network® (NCCN) guideline includes recommendations for ancillary testing. This multi-institutional study aimed to establish benchmarks for rates of adherence to NCCN guidelines.

Design: Participants reported data from molecular testing on anatomic pathology specimens, excluding hematolymphoid neoplasms, breast primary carcinomas and gynecological cytology. Each test was evaluated in its clinical and pathological context and compared against NCCN guidelines as were current during the study period (early 2013).

Results: 26 institutions reported data from 2230 testing events. In a retrospective data collection limited to colon, lung and melanoma, the most common tests performed were EGFR, ALK and KRAS; there was strict adherence to guidelines in a median 71%, with at least loose adherence in a median 95% (see table). There was adequate tissue to complete testing in a median 98% (10^{th} to 90^{th} percentile range 86-100%), though the adequacy rate for cell blocks was lower (84%, $P<.001$). Median test turnaround time was 8 days (10^{th} to 90^{th} percentile range 4-13). In a separate prospective data collection of all organ sites, the most common tests requested were EGFR, KRAS, ALK, Lynch syndrome screening and BRAF; there was strict adherence to guidelines in a median 53%, with at least loose adherence in a median 94% (see table). Adherence to guidelines was higher for lung specimens and in institutions with a higher number of multidisciplinary conferences. Pathology approval for molecular tests was required in 52% of institutions and pathologist-initiated reflex testing was offered in 57% of institutions.

Institution Percentiles	10th	25th	50th	75th	90th
Retrospective Data					
Strict adherence	33	65	71	83	90
At least loose adherence	57	91	95	99	100
Prospective Data					
Strict adherence	20	31	53	67	71
At least loose adherence	75	87	94	100	100

Conclusions: This multi-institutional study provides benchmarking data on appropriateness and timeliness of molecular testing in anatomic pathology.

2047 Whole Slide Digital Imaging Is Applicable for Routine Frozen Section Diagnosis

Kwun Wah Wen, Anna Plourde, Larry Zhao, Sarah Bowman, Grace Kim, Zoltan Laszik. University of California, San Francisco, CA.

Background: Whole slide digital imaging (WSDI) is a rapidly evolving technology with broad applications including medical education and telepathology. However, limited data exist on the use of WSDI for rendering frozen section diagnosis. We aim to validate a Philips WSDI platform for routine diagnosis in frozen sections. Here we hypothesize that diagnostic interpretation of whole slide digital images of frozen sections is not hampered to a significant extent by image quality faults and that the diagnostic potential of such digital images is comparable to that of conventional glass slide frozen section interpretation. We test our hypothesis by studying the image quality of whole slide digital images on an unbiased representative cohort of frozen sections and by assessing the spectrum of diagnostic limitations related to whole slide digital image quality deficiencies.

Design: Whole slide digital images of frozen sections from the UCSF surgical pathology archives from years 2012-2013, comprising 541 randomly selected cases with 2158 slides across all subspecialties, were evaluated for image quality and diagnostic utility. Touch preps routinely used for neuropathology cases were included. Defects identified on digital images upon initial scanning were documented and classified. For flaws on the digital images that could potentially impede the diagnosis, the slides were rescanned and reevaluated. The flaw characteristics of the images from the initial scan and rescan were recorded and analyzed for potential impact on diagnosis.

Results: Out of a total of 547 cases, only one case was deemed non-diagnostic due to image quality problems on a touch prep specimen (0.18%), corresponding to one part out of 890 parts (0.1% total parts). Although 22 additional digital images of a total of 2167 frozen sections were also classified as non-diagnostic (1.0% of total slides), a diagnosis could still be rendered on all of these cases since images of level sections were of diagnostic quality.

Conclusions: WSDI technology is applicable for frozen section diagnosis as digital images of 99.8% of cases out of a cohort of 547 unbiased randomly selected cases were interpreted as being diagnostic. We are further investigating the potential pitfalls of WSDI technology for frozen section diagnosis via in depth analysis of intra-observer diagnostic concordance in our group of pathologists.

2048 Effect of Needle Rinse Solution on Cellularity of Cellblock Preparations in Fine Needle Aspiration Biopsies

Lee Wilkinson, Haiyan Liu, Aaron Sidler, Steven Meschter, Fan Lin. Geisinger Medical Center, Danville, PA.

Background: Cellblock (CB) preparations are vital in current cytology practice. As personalized medicine requires more immunocytochemistry and molecular testing, there is increasing for highly cellular CBs. Studies have compared various protocols of CB processing; however, only limited data is available regarding effects of needle rinse solution (NRS) on cellularity. The aim of our study is to evaluate potential effects of NRSs on the cellularity of CB preparations and to assess the cost-effectiveness.

Design: 8 surgical specimens were selected, on which 4 paired fine needle aspiration biopsies (FNABs) were performed with needle rinses into 10mls of either RPMI or Cytolyt, generating 32 paired FNABs. For each FNAB, 3 passes were performed; the first yields a single air dried smear, DiffQuick stained, to evaluate adequacy, with subsequent 2 directly rinsed in either solution. The NRSs were processed via thrombin clot method to yield CBs. The H&E sections were evaluated for cellularity, measured in terms of cell clusters (>6cells in a group) and background cellularity (cells <6/cluster or single cells per average 40x field). The cellularity was compared for each paired FNAB, specimen average, and overall for RPMI vs Cytolyt. P-values were calculated using student T-test. In addition, the cost for each 10 ml aliquot (RPMI or Cytolyt) was calculated.

Results: Both CBs using RPMI or Cytolyt yield adequate cellularity. The cellularity in CBs using RPMI ranges from 11-923 cell clusters and 1-167 background cellularity. Cellularity in CBs using Cytolyt ranges from 3-1122 cell clusters and 6-188 background cellularity. The average cell clusters per specimen show a trend of higher cellularity with Cytolyt; however, only one specimen showed statistical significance (p-value of 0.039). The same is true for background cellularity, with one specimen having a p-value of 0.007. When comparing all FNABs using RPMI vs Cytolyt, cluster cellularity is not statistically significant with a p-value of 0.356, while background cellularity is statistically different with a p-value of 0.006. The cost of 10 ml aliquot is $0.88 for RPMI and $0.50 for Cytolyt.

Conclusions: Our data shows CBs using RPMI or Cytolyt yield adequate cellularity with Cytolyt trending higher than RPMI; however, the difference is not statistically significant. The cost of Cytolyt is marginally less than RPMI. With little difference in the cellularity using RPMI or Cytolyt, other factors such as specimen versatility and cost should be evaluated based on overall needs of individual laboratory when selecting an NSR.

2049 Achieving Reliability in Histology

Edward Yoon, Sergey Pyatibrat, Jeffrey Goldsmith, Kenneth Sands, Yael Heher. Beth Israel Deaconess Medical Center, Boston, MA.

Background: Specimen misidentification in the histology laboratory can result in serious patient harm. Despite efforts to abate labeling errors, incidence specifics have not been rigorously studied and standardized improvement efforts have not been reported. By utilizing tools such as root cause analysis, process mapping, quality metric assessment, and Lean methodology, we identified vulnerable steps in the histology laboratory and designed targeted improvement efforts.

Design: The study was conducted within the histology laboratory of a major academic institution with an annual specimen volume of approximately 60,000. A novel numerical step-key mapped histology workflow, facilitated error data collection, and identified the most vulnerable steps to labeling error (the root causes). Two most prevalent root causes were targeted for Lean workflow redesign: manual slide printing and microtome cutting. The initial plan-do-study-act (PDSA) cycle introduced bar-coding technology at the slide-printing step with the aim of decreasing specimen mixups by obviating the need for manual entry of accession numbers. The second PDSA cycle utilized the Lean concept of Single Piece Workflow (SPW) in the form of an innovative compartmentalized crushed ice design entitled the 'Framework to Engage and Effect Zero Errors' (iFREEZE). iFREEZE hermetically cooled, separated, and sequestered matching blocks and slides, further decreasing the incidence of specimen labeling errors.

Results: 152,952 cases were analyzed over a 31 month study period. A baseline error rate of 1% (793 errors/76,958 cases) was established prior to any systematic workflow changes over the first 15 months. Following implementation of slide printer bar coding (PDSA cycle 1), the error rate decreased to 0.3% (92 errors/32,534 cases) over the next 7 months. Following iFREEZE implementation (PDSA cycle 2), the rate was 0.2% (86 errors/43,460 cases) over the last 9 months. Overall, a 90% reduction in labeling errors has been observed since the initiation of our study.

Conclusions: Histology labeling errors can be captured in real time, attributed to a root cause, and subjected to targeted quality improvement efforts. Using relatively simple quality improvement tools, we were able to characterize and drastically reduce our institution's labeling error rate in a quantifiable manner. Our generalizable process redesign efforts have the potential to greatly improve reliability in histology as part of national and institutional patient safety goals.

Techniques

2050 Molecular Profiling of Common Melanoma Mutations – A Large Cohort Study

Nadya Al-Faraidy, Namita Deodhare, Karen Naert, Anthony Joshua, David Hogg, Marcus Butler, Suzanne Kamel-Reid, Ayman Alhabeeb, Danny Ghazarian. University of Toronto, Toronto, ON, Canada.

Background: Melanoma is one of the deadliest skin cancers. It is predicted that in 2014 alone, 6500 Canadians will be diagnosed with melanoma, of which 1050 will die. Historically, melanoma classification has been based on pathological criteria and

clinical characteristics. Recent advancements in MAPK pathway research, lead to the discovery of melanoma specific oncogenes. BRAF, NRAS and CKIT have been identified in over 50% of melanomas, posing as promising potential targets for targeted therapy. Therefore, molecular profiling for melanoma has become an important step in managing advanced cases.This study analyzes molecular characteristics of primary and metastatic melanomas presenting to UHN.

Design: A retrospective study of 1050 melanomas, from 1029 patients, at UHN, was conducted. All were melanoma cases that had undergone molecular testing for BRAF, NRAS and/or C-kit mutations in 2012-2014.For molecular analysis, DNA was extracted from formalin-fixed paraffin-embedded tissue samples. Amplification was done using the specific primers for normal and mutant alleles in exon 15 of the BRAF gene, primers for exon 1 and 2 of the NRAS gene, and primers for exon 11, 13, 17, 18 of the KIT gene. BRAF V600E/K mutations were detected using the Amplification refractory mutation system analysis. For NRAS and C-kit, PCR and sequencing were used to screen for mutations. Purified products were compared to NCBI reference sequences.Molecular results were correlated to patient's gender and anatomical site.IBM SPSS Statistics Version 21 was used for statistical analysis. Chi squared test was used to examine the association between anatomical site and mutations. $P < 0.05$ was considered significant.

Results: In the 1050 cases 78% had at least one mutation, 22% were triple negative. BRAF mutations were found in 35.1% of cases. NRAS mutations were found in 17.5%, and C-kit mutations were found in 2.6%. There was a significant relationship between mutation and anatomical site. BRAF and NRAS mutations were more prevalent on sun-exposed sites; (58.2%, 63.2% respectively). C-kit mutations showed a higher prevalence in mucosal sites (72.7%).

Conclusions: The striking large number of melanomas with at least one mutation (78% in our study) and site predilection emphasizes the significance of testing advanced melanoma cases for BRAF, NRAS and C-kit mutations. These melanoma hotspots have become readily incorporated in clinical trials. Large studies correlating molecular profiling with clinical and pathological characteristics may aid in improving personalized targeted therapy.

2051 Ki67-Adjusted Mitotic Score (KAMS) Is a Novel Prognostic Metric in Well Differentiated Pancreatic Neuroendocrine Tumors

Ritu Aneja, Sergey Klimov, Ansa Riaz, Vaishali Pannu, Shristi Bhattarai, Guilherme Cantuaria, Padmashree Rida, Michelle Reid. Georgia State University, Atlanta, GA; Northside Hospital Cancer Institute, Atlanta, GA; Emory University Hospital, Atlanta, GA.

Background: The grading of PanNETs presents numerous diagnostic challenges and limits our ability to accurately predict their clinical.behavior. Some aggressive PanNETs may appear deceptively bland while others with overt "malignant" cytology may exhibit indolent behavior. The current WHO grading system uses Ki67 index (KI) and/or mitotic count (MC) to independently obtain a histological grade (G1, G2, G3) for tumors. However there are numerous ambiguities in this grading system, including different scales of measurement of Ki67 and mitosis, sub-optimal categorical cut-offs and lack of consensus on best counting methodologies. Additionally, KI is almost always higher than MC suggesting that the latter may be unnecessary step. To fully exploit the prognosticating power of both KI and MC, we propose to rationally integrate them and derived a new metric, Ki67-adjusted mitotic score (KAMS), which represents the proportion of mitotic cells amongst cycling Ki67-positive tumor cells.

Design: Among 70 PanNETs KAMS was calculated by transforming monotonic ordinal MC into % mitotic cells and dividing it by % Ki67. Survival stratification was done via Kaplan-Meier estimator based on KAMS and KI.

Results: Using current established thresholds in PanNET grading the survival stratification for KI showed no significance between high and low Ki67 survival percentages ($p=0.768$). However KAMS was able to stratify patients into two statistically significant survival groups ($p= 0.0323$): The "above-threshold KAMS" group had 90% survival while the "below-threshold KAMS" group had a 77% survival. The ideal threshold of 1.93 was used to stratify KAMS data. Multivariate analysis revealed no significant influence of age, tumor size, lymph node invasion, peri-neural invasion and metastasis on KAMS ($p>0.2$ in all cases).

Conclusions: Low KAMS can significantly predict poor prognosis in PanNETs. This study underscores significance of our new metric, KAMS, a new metric, provides more accurate risk prediction in PanNETs, is superior to Ki67 in survival stratification and thus, could prove to be a game-changer in prognostic risk determination by identifying individuals at higher risk of progressing to metastatic disease.

2052 Comprehensive Assessment of Targetable Driver Alterations in Lung Adenocarcinomas Using a Clinical, Hybrid Capture-Based, Next-Generation Sequencing Assay

Maria Arcila, Ahmet Zehir, Donavan Cheng, Helena Yu, Marc Kris, Alexander Drilon, Gregory Riely, Michael Berger, Marc Ladanyi. Memorial Sloan Kettering Cancer Center, New York, NY.

Background: Mutation analysis plays a central role in the management of lung adenocarcinoma (LUAD). The use of multiple single gene or mutation specific assays, broadly adopted in many laboratories to detect relevant genomic alterations, often leads to delays if sequentially performed, tissue exhaustion, incomplete assessment and additional required biopsies.

More comprehensive assays based on massively parallel sequencing (NGS) offer a distinct advantage for addressing the increased testing needs of genotype-based therapeutic approaches. Here we describe our experience with a 341 gene, clinically validated hybrid-capture based NGS assay applied to testing of LUAD.

Design: Consecutive LUAD cases submitted for routine mutation analysis within a 5 month period were reviewed. Testing was performed by a laboratory developed custom hybridization-capture based assay (MSK-IMPACT) targeting all exons and selected introns of 341 key cancer genes. Barcoded libraries from tumor / normal pairs were captured and sequenced on an Illumina HiSeq 2500.

Results: A total of 142 specimens were received for testing: 23 cytology samples, 83 needle biopsies, 36 large biopsies/resections. Ten cases (7%, 10/142) did not meet suitability criteria due to very low tumor content or very low DNA yield. Failure rate was similar for cytologies and biopsies. A total of 1269 genomic alterations were detected (average 7.6 per patient, range 0-93), the majority were point mutations (71%, n=905) and amplifications (13%, n=165). The most highly mutated genes included TP53, EGFR, KEAP1 and KRAS. Copy number gains of NKX2-1 and EGFR genes and CDKN2A loss were most common. EGFR mutations and ALK fusions were detected in 24% and 1% of cases, respectively. Among the 97 EGFR / ALK WT cases, MSK-IMPACT uncovered targetable genomic alterations that would have remained undetected through focused EGFR /ALK testing alone. These included fusions in RET (12) and ROS1 (5), mutations in ERBB2 (5) and BRAF (6) and amplifications in MDM2 (1) and CDK4 (1) among others. The higher than expected rates of RET and ROS1 fusions are related to enrichment for previously tested cases known to be negative for other driver alterations.

Conclusions: Comprehensive hybrid-capture based NGS assays such as MSK-IMPACT are an efficient testing strategy for LUAD. This broad approach enables more optimal patient stratification for treatment by targeted therapeutics.

2053 Comparative Assessment of Normal B-Cells and Normal Plasma Cells for DNA Content Determination in Plasma Cell Proliferative Disorders

Aleh Bobr, Steven Bashynski, Dragan Jevremovich, William Morice. Mayo Clinic, Rochester, MN.

Background: Flow cytometry evaluation of plasma cells (PCs) is integral for the diagnosis, risk stratification, and management of patients with plasma cell proliferative neoplasms. As a part of the evaluation, DNA content of the clonal PCs is assessed by DAPI staining, and the ploidy of the clonal PCs is measured by comparing to their DNA content to that of normal PCs in the specimen to serve as an internal control. This comparison is made by calculating the ratio of the clonal PC/normal PC DNA content and reported as the DNA index. Normal PCs are used as they are most similar to the abnormal PCs, and allow for detecting abnormalities in DNA content at a threshold of 5% DNA gain or loss (i.e. abnormal PC DNA index <0.95 hypodiploid and >1.05 hyperdiploid). In clinical practice, however, there are cases in lacking normal PCs which precludes estimating DNA content by this approach. For this study, the relationship of normal B-cell DNA content to that of normal PCs was evaluated and the ability to use these cells to calculate abnormal PC DNA was explored.

Design: Data from 87 PC proliferative disorder cases was reviewed; these included cases in which the abnormal PCs were hypodiploid (n=9), diploid (n=36), hyperdiploid (n=30) and tetraploid (n=12). In each case the DNA content of the polytypic CD19 and CD45 positive B-cells was compared to that of in relation to polyclonal plasma cell population based on DAPI MFI intensity.

Results: The average DAPI MFI of the normal B-cells (50312 (±2168)was significantly lower than that of the polyclonal PCs was (52225 (±2453), ($p<0.001$) with average difference 1914 (±1245). This difference was used as a correction factor for calculating the abnormal PC DNA index using normal B-cells as the reference population. The accuracy of this new index was 94.3%. The misclassified cases were on the edge of reference range. When values ±0.1 around reference range cut off were excluded the test reached 100% accuracy in cases with diploid and hyperdiploid DNA content. The tetraploid cases required ±0.3 exclusion around reference range to reach 100% accuracy.

Conclusions: The findings help establish new way to calculate DNA content index when polyclonal plasma cells are scarce in the cases with diploid and hyperdiploid DNA content excluding DNA index values from 1.04-1.06 and in the cases of tetraploid DNA content excluding DNA index values from 1.71-1.77. The use of recalculated DNA index in hypodiploid cases requires further evaluation.

2054 Molecular Inversion Probe (MIP) Technology Generates High-Quality HER2 Copy Number Data in Formalin-Fixed Paraffin-Embedded (FFPE) Breast Cancer

Alex Bousamra, Hui Chen, Rajyalakshmi Luthra, Xinyan Lu, Ken Aldape, Rajesh Singh, Gary Lu, Ronald Abraham, Shumaila Virani, Bal Mukund Mishra, Aysegul Sahin. University of Texas MD Anderson Cancer Center, Houston, TX.

Background: MIP technology has recently proven successful in overcoming the challenges of generating high-quality copy number (CN) data from FFPE samples, requiring a minimal amount of DNA. HER2 status is currently assessed by a variety of qualitative and semi-quantitative methods, including immunohistochemistry (IHC) and fluorescence *in situ* hybridization (FISH). We hypothesized that MIP technology can provide accurate and quantitative HER2 assessment, which is especially important with the emergence of novel anti-HER2 therapies. Applying MIP technology on FFPE breast tumor tissue, we generated HER2 and pericentromeric 17 CN data by MIP and correlated them with HER2 and chromosome 17 centromere (CEP17) CN data by FISH.

Design: We selected 23 invasive breast cancers (17 with and 6 without HER2 amplification by FISH) from the archives of MD Anderson Cancer Center. For each tumor, we had previously cut 5-mm sections from a representative FFPE tissue block for IHC, FISH, and MIP array studies. Applying the ASCO/CAP 2013 guidelines for breast cancer, we performed FISH with PathVysion HER2 and CEP17 dual-probe. After manual microdissection, we extracted genomic DNA by using the PicoPure DNA extraction kit. Using the OncoScan FFPE Assay kit and OncoScan Console v1.1 (Affymetrix), we subjected DNA samples (80 ng) to genome-wide CN analysis with focus on HER2 and chromosome 17's pericentromeric region. Data were analyzed by Nexus Express for OncoScan (Biodiscovery).

Results: With a designated cut-off of 4.0 for CN gains, 16 of 17 samples (94%) had HER2 CN gains (4.0-28.0) on MIP analysis. One of 17 samples (6%) had a HER2 CN

of 2.3 by MIP (HER2 CN by FISH: 4.65; HER2 ratio: 2.12), most likely representing an admixture of tumor and stromal cells. Six of 6 tumors (100%) with negative HER2 status by FISH showed less than 4.0 CN by MIP array (1.0-3.0). All 23 samples (100%) displayed excellent correlation between CEP17 CN by FISH and pericentromeric 17 CN by MIP.

Conclusions: Our findings show a robust correlation between MIP and FISH results, with 22 of 23 samples (96%) showing similar CN data by both methods. With minimal DNA requirements using FFPE tissue, MIP array technology shows promise as a quantitative measure of HER2 CN and a more accurate representation of the tumor's HER2 status than FISH. Thus, it may become an essential tool in guiding clinical decisions regarding anti-HER2 therapy. In addition, by allowing genome-wide CN profiling, MIP technology may help improve our understanding of tumor biology and behavior.

2055 Using Nanocomposites in Fixation and Processing of Histological Material

George Burkadze, Nana Kikalishvili, Vakhtang Kargareteli. Levan Samkharauli National Forensics Bureau, Tbilisi, Georgia.

Background: During histopathologic studies an important portion of time is spent on fixation of the tissue and preparing microslides. In addition, part of chemical reagents is not safe for the environment and the personnal working in the laboratory. The purpose of the study was to optimize the fixation and processing stages using nanocomposites.

Design: In conditions of ultrasound (UP200HT) based processing we created nanocomposite fixatives using nanocomposite single layered 99% clean carbon nanotubes with modified surface, with length of 3-30 um, outer diameter of 1-4nm and inner diameter of 0.8-1.6nm. As a result of mixing nanoparticles with buffer formalin, alcohol and distilled water in different concentrations 24 nanocomposite fixatives were prepared. 208 postoperative and autopsy specimen (heart, brain, lung, etc. tissues) underwent fixation with different duration and in different temperature settings. Each experiment was double controlled using standard technique of fixation process and autolysis (ASCO/CAP. 2008). Nanocomposite reagents were also created for tissue processing purposes. We performed a comparative analysis of the materials, which underwent processing with different variations of nanocomposite-based fixatives. Final results were evaluated in hematoxilin-eosin stained slides using 5 point scoring system by four independent pathologists in blind experiment settings.

Results: Nanocomposite fixatives based on ethanol showed the best results in fixation and tissue processing – their usage reduced the standard fixation time 24 times. Nanocomposite ethanol usage for processing purposes gave a high time-effectiveness coefficient - TK - 47.5% and high effectiveness coefficient of reagent consumption - RK-33%. It means that processing of the materials needs almost twice less time and 1/3 less reagents.

Conclusions: Using nanocomposites significantly reduces the time needed for fixation and processing of the tissues as well as the volume of reagents needed. As a result it is evidently cost-effective and makes material fixation and processing more secure.

With the support of National Scientific Fund Grant – AR/303/8-315/12.

2056 A Lower Ratio of Mitotic To Proliferative Index Is Associated With Triple Negative Breast Cancer and Poor Prognosis

Guilherme Cantuaria, Sergey Klimov, Xiaoxian Li, Nikita Wright, Michelle Reid, Vaishali Pannu, Stephen Wells, Padmashree Rida, Ritu Aneja. Northside Hospital Cancer Institute, Atlanta, GA; Georgia State University, Atlanta, GA; Emory University Hospital, Atlanta, GA.

Background: Clinically important prognostic markers for breast cancer include Ki67 and mitotic indices (KI and MI), and hormone receptor status. Among these, KI is an independent prognostic marker that measures proliferation, and MI is a component of the Nottingham grading system. Both markers lack reliability for accurate disease prognosis, and are usually derived from non-overlapping fields and are quantified on different measurement scales, resulting in the loss of crucial information. In order to harness their full prognostic potential, we have extracted KI and MI from same field and on same measurement scale to determine the proportion of mitotic cells amongst proliferative cells, termed M:P ratio, which provides a measure of cell cycling kinetics within a tumor. Triple (ER/PR/Her2) negative breast cancers (TNBCs) are highly aggressive breast cancers typified by low overall survival, high recurrence and metastasis. We wanted to test if differences in M:P ratio among TNBC and non-TNBC patients can illuminate basic differences in tumor biology that can predispose certain tumors to more aggressive behavior.

Design: 4-color immunofluorescence staining was done on paraffin-embedded TNBC and non-TNBC breast tumor tissues (n=222). Phospho-histone H3 (mitotic marker, green), Ki67 (proliferation marker, blue), α-tubulin (microtubules, grey), and propidium iodide (nuclei, red). The M:P ratio was determined for each case.

Results: TNBC patients (n=59) exhibited a lower M:P ratio in comparison to grade-matched non-TNBC patients (n=163) ($p<0.05$). In addition, low stage (I and II) TNBC patients (n=39) exhibited a lower M:P ratio in comparison to stage-matched non-TNBC patients (n=99) (p=0.01). Multivariate analysis reveals no cofounding influence of age, race or hormonal receptor status on these findings.

Conclusions: Strong association of a low M:P ratio with TNBCs, suggest a surprising inherently slower cell cycling kinetics in TNBCs. Low M:P ratios in TNBCs may indicate a tumor agenda that is less "mitosis-focused" and more "metastasis-heavy". Our novel metric may thus be risk-predictive.

2057 A Novel Metric Illuminates Differences in Metastatic Risk Among Racially-Distinct Breast Tumors

Guilherme Cantuaria, Xiaoxian Li, Nikita Wright, Michelle Reid, Vaishali Pannu, Stephen Wells, Padmashree Rida, Sergey Klimov, Ritu Aneja. Northside Hospital Cancer Institute, Atlanta, GA; Emory University Hospital, Atlanta, GA; Georgia State University, Atlanta, GA.

Background: African-American (AA) women are more associated with aggressive breast tumors with higher metastatic propensity compared to European American (EA) women. While widely used as prognosticators, Ki67 index (proliferative index, PI) and mitotic index (MI), alone lack the kinetic variable, which can perhaps foretell the evolving dynamics of tumor behavior. We evaluated the MI-to-PI ratio (M:P) that represents proportion of mitotic cells amongst cycling Ki67-positive cells and its relationship to breast cancers in AA and EA patients.

Design: We employed 4-color confocal imaging on paraffin-embedded tissue slides (n=200), we counted mitotic cells (phosphor-histone H3, green) out of Ki67-positive cells (blue) from same field-of-view a-tubulin for microtubules identified specific mitotic phases, and propidium iodide stained nuclei (red).

Fig. 1

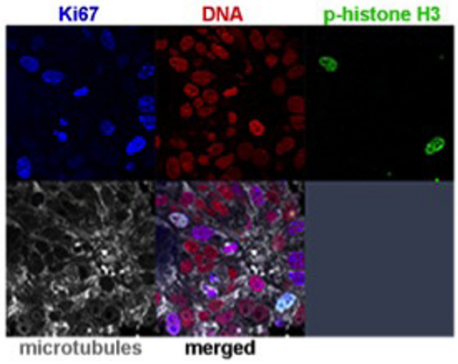

Results: Breast tumors from AA patients (n=81) exhibited a higher M:P ratio compared to grade-matched EA (n=121) patients ($p<0.01$). Early-stage (stage 1 and 2) AA patients (n=47) showed higher M:P ratio than the stage-matched EA (n=89) patients. Multivariate analysis revealed no confounding influence of age, grade, or hormone receptor status in the early stage cancers. Race is the only significant factor associated with M:P ratio. AA patients significantly correlated with an increase (p=0.04) in M:P ratio.

Conclusions: The higher M:P ratio in AA may indicate pathobiological differences in breast cancers from AA and EA patients. Further research to examine the predictive ability of M:P ratio in breast cancer prognosis is warranted.

2058 Utility of SNP Microarrays in Karyotype Normal (kn) Heme-Malignancies: A More Sensitive Approach for Investigating kn-Malignancies

Alka Chaubey, Ashis Mondal, Barbara DuPont, Kat Kwiatkowski, Eric Fung, Juan Cuevas, Amyn Rojiani, Ravindra B Kolhe. Greenwood Genetic Center, Greenwood, SC; Affymetrix, Inc, Santa Clara, CA; Georgia Regents University, Augusta, GA.

Background: Conventional cytogenetics (CC), including karyotyping and FISH, has long been the gold standard tool in the management of hematologic malignancies. These are malignancies are complex on multiple levels, & laboratory efforts over the past 3 decades have focused on better understanding of the molecular pathogenisis. The diversity of these malignancies is manifested by a wide variety of morphologic subclasses, highly varied clinical presentations, and significant variation in the responses seen clinically. One of the biggest strengths of SNP arrays is in its ability to identify copy neutral LOH (a limitation of CC) which can have grave prognostic implications for the cancer patients. Aim of the current study is to investigate the clinical utility of microarray technology in facilitating in the diagnosis, prognosis and management of cytogenetically normal hematological malignancies.

Design: We identified 42 cases (AML, MDS, PCM and ALL) which had normal karyotype and FISH. Archival reports and slides were retrieved and reviewed and clinical information obtained from patient charts. Subsequently, high resolution SNP microarray using CytoScan HD Microarray (Affymetrix Inc, Santa Clara) was performed on DNA isolated from methanol-acetic acid fixed bone marrow pellets.

Results: In our study all the kn-malignancies showed multiple genomic abnormalities. inculding Copy number gains and losses in all sub types (AML/MDS, ALL, MF ALL, PCM) which identified pathogenic and likely pathogenic deletions involving cancer genes. Interestingly 3 cases (CMML, ALL and MF) identified whole chromosome arm LOH findings consistent with the pathogenesis of the neoplastic disorder.

Conclusions: Advancements in microarray technologies are giving us an opportunity in marking and measuring the leukemic population in determination of minimal residual disease (MRD). The technology even offer a first-order assessment to discriminate between patients with drug-sensitive disease who might be cured with traditional cytotoxic chemotherapy, possibly use lower total doses, and those with inherent drug-resistant leukemia who will not be cured. In addition, it allows us to characterize individual leukemias by molecular profiles that not only relate to clinical behavior but also provide potential targets to direct therapeutic strategies. By merely looking at the karyotype/FISH or few mutations (c-kit, NPM1, FLT3-ITD, IDH1, etc), this assessment is incomplete.

2059 A Novel Quantitative IHC (qIHC) Method for Precise Measurements of Expressed Proteins Directly in FFPE Specimens

Helene Derand, Rikke Krusenstjerna-Hafstrom, Jesper Lohse, Kenneth Petersen, Hans Christian Pedersen, Kristian Jensen. Dako, Glostrup, Denmark.

Background: In routine pathology, in situ quantification of protein in formalin-fixed, paraffin-embedded (FFPE) tissue is limited to immunohistochemistry (IHC) which is semi-quantitative at best. There is a general need to make pathologic examinations less subjective and to support the accuracy required for companion diagnostics. We have developed a new reliable quantitative IHC (qIHC) method based on a novel amplification system that enables quantification of protein directly in FFPE tissue by counting dots using a standard bright field microscope.

The goal of this study was to assess the analytical performance of qIHC in a HER2 assay analyzing both FFPE cell pellets and breast cancer specimens. Furthermore, qIHC can be combined with traditional IHC and examples will be demonstrated.

Design: Five different cell lines with HER2 expression ranging from undetectable with IHC to strongly positive (IHC 3+) were used as test samples. Flow cytometry, and ELISA were used as reference methods to confirm protein expression levels and stability of the cell lines. The qIHC assay was conducted using an automated Autostainer Link 48 stainer.

In addition, breast cancer specimens were stained to compare standard HER2 IHC with qIHC, and on brain tumor specimens qIHC was combined with IHC.

Results: Repeatability, reproducibility, robustness, linearity, sensitivity, and quantification limits were evaluated and each of the different tests showed statistical significant results (p: <0.0001–0.005). The dynamic range, linearity and sensitivity of the assay were investigated by correlating the qIHC results to a flow cytometry assay as well as an FDA-approved ELISA kit for HER2 measurement. All tests demonstrated statistically significant correlation (p: 0.0002–0.0045).

The comparison of qIHC and HER2 IHC on 44 breast cancer specimen was successful and a strong correlation was confirmed between IHC and qIHC (p: <0.0001).

Conclusions: The results demonstrated ability of qIHC to measure Her2 accurately and precise within a large dynamic range (covering 3 log scales). Compared to standard IHC, the qIHC Her2 assay were able to quantify protein expression levels both well above as well as below current Her2 IHC assays, using only a single assay.

In this work we have demonstrated that qIHC is a novel, versatile brightfield based quantitative technology which can quantify protein directly in FFPE tissue.

2060 Sequential Dual Immunocytochemistry Staining Technique in Limited Cytology Specimens

Christina DiCarlo, Jan Silverman. Allegheny General Hospital, Pittsburgh, PA.

Background: Immunocytochemistry (ICC) is typically performed on cell blocks from FNA cytology specimens. However, cell blocks may lack sufficient cellularity, limiting conventional immunostaining. The goal of this study is to provide an alternate ICC technique on Papanicolaou (Pap)and/or Diff-Quik (DQ) stained slides when a cell block lacks adequate cellularity.

Design: Sequential ICC was performed on both alcohol-fixed Pap and air-dried DQ stained touch preparations containing adequate tumor cells from 18 cases. An anticipated negative ICC stain was first applied to the slides and analyzed. If the expected negative staining results were found, a second stain that was expected to be positive was applied to the same slide. The following first and second sequential stains were applied for adenocarcinomas (AC) at the following sites: TTF-1 or PAX-8 vs. GATA-3 for breast (6 cases), p63 vs. TTF-1 for lung (4 cases), GATA-3 or TTF-1 vs. PAX-8 for ovary/endometrium (3 cases), and GATA-3 vs. CDX-2 for colorectum (2 cases). Squamous cell carcinoma (SCC) of the lung (3 cases) was sequentially stained with TTF-1 vs. p63. Positive immunostaining was defined as ≥ 1% staining of tumor cells.

Results: A total of34 slides (19 Pap and 15 DQ) underwent sequential ICC. Only 7 slides (20.6%) were unable to undergo the second round of stains after the first round due to the following: lack of adequate cellularity [6 slides, 17.6%], and nonspecific positive staining (1 slide, 2.9%). Of the 27 slides that completed two rounds of staining, 15 slides (55.6%) had expected staining patterns (first stain negative/second stain positive), 11 slides (40.7%) had negative first and second staining and only 1 slide (3.7%, Pap) lost adequate cellularity after the second stain. When analyzing results by type of carcinoma, 100% of ovarian AC slides (4/4) had expected staining patterns. The remaining carcinoma types had expected staining results as follows: 80% (4/5 slides) for lung (AC), 75% (3/4 slides) for lung (SCC), 50 % (2/4 slides) for colorectum (AC), 28.6% (2/7 slides) for breast (AC), and 0% (0/2 slides) for endometrium (AC).

Conclusions: 1. The majority of slides (79.4%) maintained adequate tumor cellularity and therefore, completed the sequential ICC process. Of these slides, 55.6% had expected staining patterns. Despite limitations in sample size, carcinoma of the ovary and lung stained more accurately than those of the breast, colorectum or endometrium. 2. Dual sequential ICC staining on cytologic smears is an alternate technique when cell blocks are not available or have limited cellularity in the work up of FNA specimens.

2061 Detection of Mutant Circulating Tumor DNA (ctDNA) in Plasma of Patients With Colorectal Cancer (CRC)

Juliane Dworniczak, Christiana Rossenbach, Simone Reisch, Christian Hart, Laszlo Fuzesi, Barbara Dockhorn-Dworniczak, Bernd Dworniczak. Technical University Munich, Munich, Germany; Institute of Pathology, Kempten, Germany; Klinikum Kempten, Kempten, Germany; University Hospital of Muenster, Muenster, Germany.

Background: New biomarkers associated with tumor initiation and progression have become available for molecular characterization of human cancer and are used for diagnostic, prognostic and predictive purposes. However, monitoring of tumor burden and response to treatment in CRCs is still assessed by imaging diagnostic techniques and the use of protein biomarkers with limited sensitivity and specificity. Several reports have shown that analysis of cell free DNA (ctDNA) uncovers personalized biomarkers for monitoring cancer patients.

Design: To implement this technique into a routine clinical laboratory we started a pilot study with CRC patients. Optimization and normalization of the workflow covers all aspects of the procedure: blood sampling, isolation of the ctDNA, determination of its entire concentration and the tumor-derived portion, its fragmentation and optimized storage. CtDNA is enriched by cold-PCR and tumor derived mutations are either verified by deep sequencing or by qPCR.

Blood sample from CRC patients (stage I-IV) were collected before surgical treatment at primary diagnosis, 5 days after operation and during postoperative oncological monitoring. From patients treated with neoadjuvant chemoradiation blood samples were obtained before and during treatment procedures. To validate the results respective tumor DNA is sequenced by use of a gene panel (Qiagen-SABiosciences) containing 20 tumor genes known to be frequently mutated in colon cancer.

Results: Tumor tissue material and the corresponding blood plasma were analyzed from 20 CRC patients with localized (10) and metastatic disease (10) using our gene panel. For patients with advanced stage and mutation positive tumors it could be shown that in most cases the clinical relevant mutations in the *RAS* and the *BRAF* gene could already be detected in plasma at the time of the primary diagnosis. In contrast patients with localized disease have detectable ctDNA in less than 50%. So far mutations identified in plasma samples were always identical to the mutation pattern in the primary or metastatic tumor tissues. Detectable ctDNA levels in advanced stages were found even under therapy up to 6 months of follow-up.

Conclusions: Our data show that, although analyses of liquid biopsies are challenging - its implementation is feasible in a well equipped clinical laboratory; we are sure that in future its use will be a cornerstone in personalized medicine.

2062 Effect of Decalcification on Immunohistochemistry Performance

Philip Ferguson, Yolanda Sanchez. St. Bernards Medical Center, Jonesboro, AR; Leica Biosystems, Buffalo Grove, IL.

Background: Deleterious effects of decalcification on immunohistochemical (IHC) and in situ hybridization (ISH) stains performed on formalin fixed paraffin embedded tissues are a well known in the anatomical pathology laboratory. This study compares the performance of three commonly used decalcification solutions on multiple tissue types for varying lengths of decalcification.

Design: Multiple IHC antibodies including AE1/AE3, CD2, CD3, CD3, CD5, CEA, CK20, ER, and SMM-HC were compared using different tissue types (gallbladder, colon, kidney, tonsil, skin, uterus, and liver). Tissue was selected from completed surgical pathology cases, in which the patient information was blinded, and in accordance to local institutional IRB approval. Tissue sections were decalcified for 0, 1, 2, and 24 hours in each solution, and tissue microarrays (2mm punch cores) were constructed to evaluate relative performance of each stain on the same slide. IHC staining was performed on the Leica Bond III® automated staining platform.

Results: The three solutions showed decreasing intensity of staining as time progressed in decal solution up to 24 hours before processing. Formical 2000 had a higher average of staining intensity at 5.6, Immunocal second at 5.1, and EDTA last at 5.0. This average was for all results combing all of the times, tissue types, and antibodies for brevity. Some antibodies were affected more than others by decalcification (data not shown).

Conclusions: As expected decalcification showed deleterious effects on IHC staining. Formical 2000 showed the overall best performance with Immunocal second, and EDTA third.

2063 Effects of a Multi-Disciplinary Approach To Improve Volume of Diagnostic Material in CT-Guided Lung Biopsies

Philip Ferguson, Catherine Sales, Dalton Hodges, Elizabeth Sales. St. Bernards Medical Center, Jonesboro, AR; Doctors' Anatomic Pathology Services, Jonesboro, AR.

Background: Recent publications have emphasized a multidisciplinary approach for maximum conservation and utilization of lung biopsy material. This paper quantifies the effect of a multidisciplinary (pathology, radiology, and oncology) strategy implemented in late 2008 to optimize and increase tissue volume in CT guided lung biopsies (TNCB). The strategy was three-pronged: (1) if safe for patient, perform additional biopsy passes after obtaining diagnostic material, (2) place biopsy material in multiple cassettes, and (3) conserve all tissue ribbons when cutting blocks in the histology lab. This study quantifies the effect of recommendations #1 and #2.

Design: TNCB from 2007 (pre-multidisciplinary approach) were compared to 2012 (post-multidisciplinary approach implementation) as part of a retrospective analysis. Patient medical records were reviewed and main variables analyzed include: biopsy length (measured to nearest 0.1 cm on microscopic slide), number of blocks submitted, diagnosis, and complications. Biopsy needles (Bard 20 gauge) used between 2007 and 2012 were unchanged, and the biopsy length measured was considered to be directly proportional to tissue volume in the block.

Results: Biopsy length increased 2.4 fold while the complication rate (chest tube placement) decreased 49%. No other major complications were identified. Number of cases with at least 2 blocks available for testing increased from 11% to 96%.

	2007	2012
No. of Cases:	130	150
No. of Tissue Blocks:		
1	112 (88.9%)	6 (4.0%)
2	13 (10.3%)	144 (96%)
3	1 (0.7%)	0 (0%)
Total Biopsy Length:		
Minimum	0.1 cm	0.4 cm
25% Percentile	0.6 cm	1.5 cm
Median	1.0 cm	2.3 cm
75% Percentile	1.3 cm	3.0 cm
Maximum	3.9 cm	6.8 cm
Mean	1.0 cm	2.4 cm
Std. Deviation	0.6 cm	1.2 cm
Complications: Chest Tube Placement	17 (13.1%)	10 (6.7%)

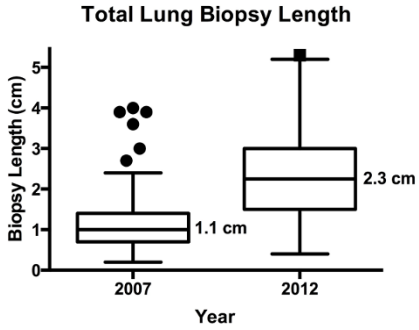

Conclusions: The effect of our multidisciplinary approach to CT guided lung biopsies was effective in significantly increasing tissue volume and number of available blocks for testing with an apparent decrease in the complication rate.

2064 A Rapid Multiplex Mass Spectrometry Assay for Mutational Profiling of Colorectal Cancer

Kenneth Friedman, Virginia Breese, Shaolei Lu, Howard Safran, Kimberly Perez, Cynthia Jackson, Shamlal Mangray, Murray Resnick, Evgeny Yakirevich. Rhode Island Hospital and The Warren Alpert Medical School of Brown University, Providence, RI.

Background: As the number of selective therapeutic targets in colorectal cancer (CRC) continue to expand, there is a need for a high throughput genotyping method that can evaluate multiple mutations simultaneously in clinical cancer specimens. While next generation sequencing provides comprehensive coverage, variants of unknown significance hinder streamlined clinical use. We analyzed the performance of a colorectal panel that has been designed and validated in our laboratory for multiplex mass spectrometry genotyping assay.

Design: Fifty-six colorectal adenocarcinoma samples submitted for molecular testing as part of routine patient care were tested. Twenty-seven tumors were microsatellite stable (MSS), and 29 were microsatellite unstable (MSI). A unique colorectal carcinoma panel was custom designed to include 240 mutations within 16 genes *(KRAS, BRAF, NRAS, ERBB2, ERBB3, PIK3CA, PTEN, TP53, MLH6, MLL3, APC, CTNNB1, FBXW7, SMAD4, TGFBR1, TGFBR2),* representing the most common and clinically relevant mutations in CRC as catalogued in COSMIC. A total of 230-460ng of DNA extracted from FFPE specimens was analyzed by multiplex mass spectrometry genotyping assay (Sequenom). All newly identified mutations were verified by Sanger sequencing or an alternative Sequenom method.

Results: A total of 134 mutations were identified in 51 of 56 cases. Mutation frequency varied from 1-6 with an average of 2.63 mutations per tumor. Mutations were most common in *KRAS* (34%), *TGFBR2* (30%), *BRAF* (29%), *TP53* (27%), *MLL3* (23%), *APC* (20%), *PIK3CA* (18%), and *PTEN* (13.8%). Lower frequency mutations were identified in *ERBB3* (11%), and *ERBB2* (4%). Sixteen cases contained previously identified *KRAS* mutation and 12 cases had *BRAF* mutations, all of which were also detected by the Sequenom assay with no false positives. Of note, 14 of 16 *KRAS* mutated cases (87%) and all *BRAF* mutated cases harbored at least one additional mutation in another gene. Mutations in *KRAS* were significantly more frequent in MSS tumors (P<0.0001). Mutations in *BRAF*, *TGFBR2, MLL3*, *MSH6,* and *PTEN* were strongly associated with MSI tumors (P<0.02).

Conclusions: Our comprehensive panel for detecting genomic alterations in CRC is robust in that it detected mutations with similar frequency to publicly available data. It also uncovered an unexpectedly high frequency of mutations in genes with an unclear but evolving significance in colorectal carcinogenesis (eg, *MLL3*, *TGFBR2*). Continued use in the clinical setting has the potential to unearth new associations and pathways amenable to treatment.

2065 Simultaneous Detection of Mirna21 and Mirna205 in Breast Cancer Tissue By a Novel Magnetobiosensor

Rosario Granados, Susana Campuzano, Rebeca Torrente-Rodriguez, Eva Lopez-Hernandez, Juan Dominguez-Canete, Jose Pingarron, Jose Sanchez-Puelles. Hospital Universitario de Getafe, Getafe, Madrid, Spain; Universidad Complutense de Madrid, Madrid, Spain; Centro de Investigaciones Biológicas, Madrid, Spain.

Background: Up-regulation of some microRNAs (miRs) such as miR-21, has been associated with poor prognosis in breast cancer. MiR-205 is reduced in breast cancer, and seems related to tumor agressiveness. Simultaneous detection of miR-21 and miR-205 may allow further understanding in the contribution of miRNA dysregulation to the behaviour of breast cancer. The use of a novel magnetobiosensor for the rapid and simultaneous detection of miR-21 and miR-205 is described.

Design: An electrochemichal nucleic acid biosensor using antimiR-21 and antimiR-205 probes and chitin-modified magnetic beads with p19 viral protein, was developed. Simultaneous measurements of miR-21 and miR-205 were performed with 1 mcg of RNAt extracted from fresh tumor and from non-tumoral tissue in 5 breast carcinomas. The same approach was used for metastatic breast-cancer cell lines. Measurements were applied to primary epithelial nontumorigenic cells as a control.

Results: Three of the breast tumors analyzed were ER and PR positive and two were triple-negative (TN) tumors. The fifth one was ER, PR and HER2 positive. Overexpression of miR-21 and underexpression of miR-205 was seen in a metastatic breast cell line and in 3 breast cancer tissues. Their expression of miR-21 and miR-205 ranged from 704 to 1609 nA and from 375 to 429 nA respectively. Normal breast tissue had miR-21 vaues of 442nA and miR-205 of 1187 nA. The two TN tumors had elevated miR-21 (923 and 1014 nA) but no significant reduction of miR205 (875 and 1058 nA). The HER2 positive tumor had the most striking difference in miR expression (1609 nA for miR-21 and 375 for miR-205). Amperometric measurements obtained in solutions with different miR-21 and miR-205 mixtures revealed no significant cross-talking, proving the viability of the dual magnetosensor for the simultaneous detection of both miRs.

Conclusions: A novel magnetobiosensor is capable of dual quantitative measurement of miR-21 and miR-205 in breast cancer tissue and cells with high sensitivity and specificity. MiR-21 was elevated in all tumor samples from fresh breast cancer tissue and cell lines, while miR-205 showed underexpression in cells and in most tissues analyzed. Dual measurement of these tumor progression and agressiveness markers by this automated, short and cost-effective assay, constitutes an important methodological advance that may permit further insights in breast cancer behavior.

2066 Comparative Study in the Interpretation of FISH HER2, 2007 and 2013 Guidelines in Breast Cancer

Juan Pablo Gutierrez, Natalia Vilches, Oralia Barboza, Hersilia Hernandez Zamonsett, Raquel Garza. Hospital Universitario, Monterrey, Nuevo Leon, Mexico.

Background: The 2007 ASCO/CAP interpretation guideliness for FISH dual HER2 test considered a positive test with a FISH HER2 / CEP17 ratio 2.2 or greater.Equivocal with a FISH HER2 / CEP17 ratio 1.8 –2.2 ; and negative when the FISH HER2 / CEP17 <1.8. In 2013 a change in the ASCO / CAP interpretation parameters in the guideliness, consider now a HER2/CEP17 ratio ³2 and also a HER2/CEP17 ratio <2.0, with an average HER2 copy number ≥6.0 signals/cell as a positive test. When a HER2/CEP17 ratio <2.0, but with an average HER2 copy number <6.0 signals/cell is considered as an equivocal ISH, and a HER2/CEP17 ratio <2.0, but with an average HER2 copy number ≥4.0 signals/cell is considered as a negative ISH.

Design: 2908 cases of breast cancer were included, using the diagnostic criteria of the ASCO / CAP 2007 compared to the 2013 guidelines for FISH / Her2 test. Also a total of 1388 (45.67%) cases with hormonal receptors which were interpreted accordingly to the ASCO/CAP 2010 guideliness were compared.

Results: There was an increase in positive Her2 cases from 2007 vs 2013 criteria showing a total of 961 (31.6%) positive cases vs 1014 (33.37%) positive cases respectively. A decrease in negative cases was found showing a total of 1935 (63.6%) negative cases using 2007 criteria versus 1762 (57.99) negative cases with the 2013 criteria, as well an increase in equivocal cases was found showing 15 (0.39%) cases using 2007 criteria vs 130 (4.2%) cases using the 2013 criteria. In the cases with hormonal receptors the following differences were determined accordingly to the HER2 result comparing 2007 vs 2013 guideliness ER + / HER2- 647 (46.61%) vs 598 (43.08%), ER + / HER2 + 190 (13.68%) vs 206 (14.84%), RE / Her2 + 227 (16.35%) vs 241 (17.36%), RE / Her2 259 (18.65%) vs 234 (16.58%). Non classified for a equivocal FISH HER2 9 (0.64) vs 60 (4.32%).

Conclusions: The changes observed in this study between the interpretation guideliness , showed an increase in Her2 positive and equivocal cases by FISH in 2013 ASCO / CAP interpretation. Also in the comparison between hormonal receptors, an increase in RE+/Her2+, RE-/Her2+ cases and a decrease in triple negative cases.

2067 Quantum Dot IHC as a Method To Characterize Mast Cells

Ellen Hatch, Diane Lidke, Tracy George. University of New Mexico, Albuquerque, NM.

Background: Immunohistochemistry (IHC) is a well-established method that allows for identification of antigens indicative of cell type and origin. Currently, fluorescence is an attractive alternative to enzyme-linked chromophores since fluorescence provides quantitative information and allows for higher resolution imaging. In particular, fluorescent nanoparticles, or Quantum Dots (QDs), have been exploited for IHC since they offer a range of spectrally distinct probes for multiplex analysis. Here, we have used QD-based IHC (QD-IHC) to characterize and quantify biomarker expression in mastocytosis.

Design: The QD-IHC protocol is designed to closely mirror standard IHC procedure using formalin-fixed samples with standard techniques for antigen retrieval. Current targets include tryptase, CD117, CD25 and CD30. Initial antibody screening is

performed using two-step labeling with unlabeled primary antibodies followed by QD-labeled secondary antibodies. Ultimately, QDs are directly conjugated to primary antibodies using click chemistry (Invitrogen). Imaging is performed using a Nikon TE2000 equipped with a CRI Nuance spectral imaging CCD camera. Spectral images are then unmixed using either the Nuance software or Matlab scripts developed in-house.
Results: Fig 1 shows aggressive systemic mastocytosis in spleen with tryptase (green), CD25 (red), and autofluorescence (white) using QD-IHC, shown as an unmixed image.

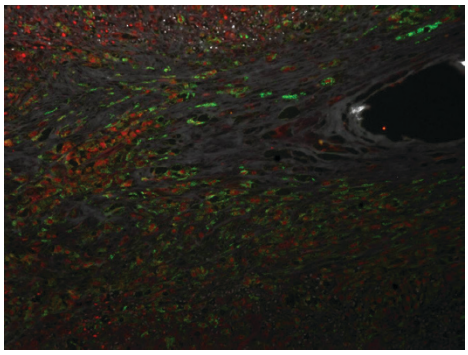

Fig 2 shows the spectral signature of CD25 expression in mast cells across the entire slide, normalized to tryptase levels.

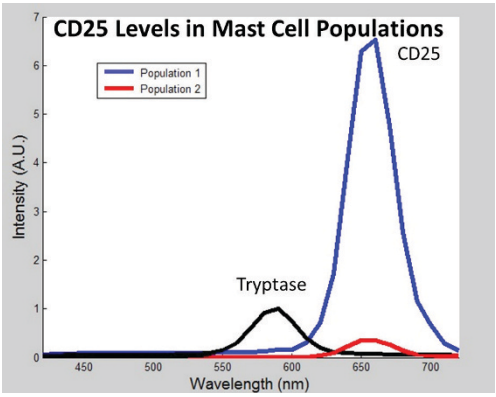

Conclusions: We have used multiplex QD-IHC to quantitatively examine biomarker expression on mast cells in aggressive systemic mastocytosis. QD-IHC allows for detailed information about mast cells in health and disease which can help us understand pathogenesis and provide targets for diagnosis and therapeutics.

2068 Application of HER2 CISH PharmDXTM for DNA Ploidy Determination

Mai He, Terese Pasquariello, Margaret Steinhoff. Women & Infants Hospital of Rhode Island, Providence, RI; Alpert Medical School of Brown University, Providence, RI.
Background: Products of conception (POC) study is encountered daily in general pathology practice and molar workup is an important part of the examination. Ploidy analysis, expressed as DNA index (DI), is part of the pathological workup of molar pregnancy. DI can be assessed by means such as flow cytometry (FC) measurement of DNA content at different phases of cell cycle, by interphase fluorescence in situ hybridization (FISH) or by cytogenetics. These techniques require specific equipment other than the regular light microscope, or tissue requirement other than formalin-fixed, paraffin-embedded (FFPE) tissue. Chromogenic in situ hybridization (CISH) is becoming a popular way to detect *HER2* gene amplification in many pathology labs. This study aims to determine whether HER2 CISH assay can be used to determine DI in POCs.
Design: HER2 CISH pharmDx™ Kit (Dako, SK109, Carpinteria, California) is a direct dual-color assay for quantitatively determination of *HER2* gene amplification in FFPE breast cancer tissue specimens. This kit generates red (HER2) and blue (CEN-17) chromogenic signals on the same tissue section, which can be evaluated by bright field microscopy. For each case, signals are counted in twenty nuclei. Twenty-two (22) POC cases were chosen from the departmental archives, including 6 complete hydatidiform mole (CM), 10 partial mole (PM) and 6 hydropic POC (HP). CISH assay was performed and compared to DNA index obtained by FC and p57 immunohistochemistry (IHC).
Results: In the ten triploid PM cases, CISH generated HER2 signal value 2.925+/-0.19. Nine cases (90%) had values within this range, except one case (2.5). In diploid cases, CISH generated HER2 signal value 2.063+/-0.19. Results from eleven (91.7%) cases fell within this range, except one HP case (2.35). Sensitivity is 90%, specificity 91.6% and overall accuracy 90.9%.
Conclusions: Her2 CISH can be used as a DNA index marker in the molar workup of POC specimen. Concurrent CEN-17 can be used as internal control in case of HER2 amplification. This assay can be performed in any lab that can perform IHC.

2069 Expanded Targeted Panels Increase the Likelihood of Identifying Actionable Mutations

Douglas Hinerfeld, Grace Stafford, Christopher Potter, Guruprasad Ananda, Gregory Tsongalis, Susan Mockus. The Jackson Laboratory for Mammalian Genomics, Bar Harbor, ME; The Jackson Laboratory for Genomic Medicine, Farmington, CT; Geisel School of Medicine at Dartmouth and Dartmouth-Hitchcock Medical Center, Lebanon, NH.
Background: Most targeted gene panels currently in clinical use are capable of identifying actionable gene variants in a small select gene list. The advantage of larger targeted sequencing panels is the increased probability of identifying an actionable gene variant in additional genes. This hypothesis was tested using a 358-gene panel for the identification of actionable gene variants that would not be identified in smaller and more commonly used gene panels.
Design: DNA from 51 solid tumor FFPE samples was sequenced on Illumina HiSeq 2500 or MiSeq sequencers using a CLIA-certified 358-gene targeted sequencing assay. FASTQ files generated from Illumina's CASAVA software were submitted to a Clinical Genome Analytics (CGA) data analysis pipeline to perform automated read quality assessment, alignment, and variant calling for SNPs, in/dels, and CNVs. Clinical reports were generated for each sample and actionable variants were compared for inclusion on the 50-gene Ion AmpliSeq and 48-gene TruSeq Amplicon cancer panels.
Results: An average of 3 actionable gene variants were identified from a targeted sequencing assay of 358 genes in 51 solid tumor biopsies. The average therapeutic options consisted of 1.4 FDA approved drugs in the patient's tumor type, 8.8 FDA approved drugs in another tumor type, and 12 investigational drugs across an average of 73 clinical trials. Actionable gene variants not commonly found on smaller panels included AURKA F31I, ERBB3 A232V, FGFR4 G388R, MAP2K1 P124S, and MYC amplification. Each of these variants were targeted by a drug that was in an actively recruiting clinical trial, at the time of clinical report generation.
Conclusions: Larger, targeted NGS gene panels increase the likelihood that an actionable mutation will be identified. This expands the treatment options for the oncologist and is likely to benefit patients that have exhausted standard of care options.

2070 Validation of a Next Generation Sequencing Based 358 Gene Cancer Panel Assay for the Detection of Actionable Mutations in FFPE Tumor Samples

Douglas Hinerfeld, Guruprasad Ananda, Susan Mockus, Micaela Lundquist, Vanessa Spotlow, Al Simons, Talia Mitchell, Grace Stafford, Vivek Philip, Timothy Stearns, Krishna Murthy Karaturi, Karen Rasmussen. The Jackson Laboratory for Genomic Medicine, Farmington, CT; The Jackson Laboratory for Mammalian Genomics, Bar Harbor, ME; The Mount Desert Island Biological Laboratory, Bar Harbor, ME.
Background: The continued development of targeted therapeutics for cancer treatment requires the parallel development of more complex methods for the molecular profiling of the patient's tumor. This has resulted in the development of next generation sequencing (NGS) cancer gene panel assays in CLIA certified laboratories for the purpose of somatic mutation detection. We describe the validation of a 358 gene NGS-based molecular diagnostic assay that detects clinically actionable somatic mutations in solid tumors to inform the selection of targeted therapeutics for cancer treatment.
Design: Using a combination of clinical FFPE samples, FFPE control samples harboring actionable mutations at known allele frequencies, and publicly-available benchmark datasets, the accuracy (comparison with an external CLIA-certified assay), precision (repeatability and reproducibility), sensitivity (comparison with HapMap and HorizonDx reference standards) and specificity (confirmation with an alternative technology like PCR or NanoString) of our assay was determined. For clinical samples, DNA was purified from macrodissected unstained sections of FFPE tissue followed by NGS library construction. Using hybrid capture, the 358 genes of interest were enriched and sequenced on the Illumina HiSeq 2500 or MiSeq sequencers followed by variant detection and functional and clinical annotation for the generation of a clinical report.
Results: Actionable variants were detected in the form of single nucleotide variations and small insertions and deletions (≤50bp) in specimens with a neoplastic cell content of ³10%. The assay was also validated for the detection of clinically actionable gene amplifications.
Conclusions: Using a variety of clinical and well-characterized samples, we successfully validated our assay for the detection of actionable mutations that support the identification of new therapeutic options for patients who have failed traditional treatment modalities.

2071 Potential Pitfalls in the Detection of BRAF V600E Mutation By Immunohistochemistry

IVY John, Alfredo Valente, Jamie Tull, Charlene Maciak, Shengle Zhang. SUNY Upstate Medical University, Syracuse, NY.
Background: Immunohistochemistry (IHC) with antibody (VE1) against *BRAF* V600E mutant protein is a relatively new technique that is increasingly used as an alternative to the more time-consuming and labor-intensive PCR-based molecular assay. However, various patterns of non-specific IHC staining with antibody VE1 have been encountered in our practice. These may represent potential pitfalls in the interpretation of IHC results.
Design: We performed IHC with antibody VE1 against *BRAF* V600E on 53 cases that were previously validated by real-time PCR. These included 17 papillary and follicular thyroid carcinomas, 20 melanocytic lesions, 11 lung and 4 colorectal adenocarcinomas. IHC with VE1 antibody (Spring Bioscience, 1:50) was performed according to the manufacturer's instructions using brown or fuchsin red chromogen. Staining intensity was graded as follows: positive (2+, 3+), negative (-) or equivocal (1+). The staining characteristics, including homogeneity, granularity, intracellular location, and distribution in lesional and normal tissues were evaluated.

Results: Diffuse and homogenous cytoplasmic staining, with or without superimposed granular staining and staining intensity of 2+ or more, strongly correlated with real-time PCR and is therefore considered specific staining. Granular and/or nuclear staining, staining of luminal secretion, colloid and/or macrophages were all non-specific. 25/27 (93%) of the negative cases confirmed by PCR showed non-specific staining, including weak to moderate granular cytoplasmic staining in all cases, moderate to strong nuclear staining in 7/25 (28%), and secretion, colloid and/or macrophage staining in 4/25 (16%). Non-specific nuclear staining was seen exclusively in lung and colorectal adenocarcinomas, and occasionally in normal colonic mucosa. IHC with brown and fuchsin red chromogen showed comparable staining patterns.
Conclusions: Non-specific staining is commonly encountered when using *BRAF* V600E (VE1) IHC. Knowledge of these staining patterns is necessary to avoid misinterpretation of these patterns as positive results.

2072 RNA Based Next Generation Sequencing (NGS) Assay To Detect Gene Fusions in Translocation Associated Sarcomas

George Jour, Ryma Benayed, Catherine OReilly, Marc Ladanyi, Maria Arcila. Memorial Sloan Kettering Cancer Center, New York, NY.
Background: Translocation associated (TA) sarcoma diagnosis relies on identification of specific gene fusions. Traditional detection methods, such as RT-PCR and fluorescence *in situ* hybridization (FISH) are labor intensive and have limitations in sensitivity, scalability, multiplexing and detection of novel fusions. Herein, we explore the performance of the Archer anchored multiplex sarcoma panel as a novel NGS fusion detection solution in TA sarcomas.
Design: RNA was isolated from 4 sarcoma cell lines and 7 clinical samples. Total nucleic acid was isolated from FFPE samples using the Agencourt Formapure™ kit. RNA was isolated using a Trizol-based protocol. Libraries were prepared using Archers Anchored Multiplex PCR (AMP™) method using a set of gene-specific primers targeting exons in the sarcoma genes of interest.

Target Gene	Targeted exons	Direction
ALK	19,20,21,22	5'
CAMTA1	7,8,9,10	3'
CCNB3	4,5,6	3'
CIC	19,20	3'
CSF1	5,6,7	3'
EPC1	9,10,11	3'
EWSR1	7,8,9,10,11,12,13,14	5'
EWSR1	4,5,6,7,8,9,10,11,12,13,14	3'
FOXO1	1,2,3	5'
FOXO1	1,2,3	3'
FUS	5,6,7,8,9,14,15	5'
FUS	4,5,6,7,8,9,10,11,12,13,14	3'
GLI1	4,5,6,7	5'
GLI1	4,5,7	3'
HMGA2	1,2,3,4,5	5'
HMGA2	1,2,3,4,5	3'
JAZF1	2,3,4	3'
MEAF6	4,5	3'
MKL2	11,12,13	3'
NCOA2	11,12,13,14	3'
NTRK3	13,14,15,16	5'
NTRK3	13,14,15	3'
PDGFB	1,2,3	5'
PLAG1	1,2,3,4	5'
PLAG1	1,2,3	3'
SS18	10,11	5'
SS18	4,5,6,8,9,10	3'
STAT6	1,2,3,4,5,6,7,16,17,18,19	3'
TAF15	6,7	5'
TAF15	5,6,7	3'
TCF12	4,5,6	3'
TFE3	3,4,5,6	5'
TFE3	3,4,5,6	3'
TFG	6	5'
TFG	4,5,6,7	3'
USP6	1,2,3	5'
YWHAE	5	3'
FAM22A(NUT2MA)	2	5'
FAM22B (NUT2MB)	2	5'

Final libraries were sequenced on Illumina MiSeq as 2x150bp paired-end reads. Analysis was performed using the Archer™ automated analysis pipeline V2.0. Results were compared to conventional methods including FISH, RT-PCR and/or DNA capture-based NGS assay, when available.
Results: The translocations identified in tested samples, along with analytical parameters, are summarized below.

Sample ID	Expected Translocation (sarcoma subtype)	Identified translocations	Supporting number of split reads/ (% split reads)	Total reads / (% reads with MBC)	Unique fragment reads (UFR)/ % RNA UFR	% Unique fragments mapped on target	RNA mean fragment length	RT-PCR	FISH	NGS
Cell line 1	EWS-FLI-1 (Ewing Sarcoma)	EWS-FLI1 (Ex7/Ex9)	944/100%	2.13M/97%	235K/44%	61.2 %	141bp	Pos	NA	NA
Cell line 2	EWS-WT1 (Desmoplastic small round cell tumor)	EWS-WT1 (Ex7/Ex7)	3911/99.6%	165K/82%	41K/97%	5.2%	170bp	Pos	NA	NA
Cell line 3	SS18-SSX1 (Synovial sarcoma)	SS18-SSX1 (Ex9/Ex7)	511/77.9%	1.83M/95%	256K/98%	48.63%	130bp	Pos	NA	NA
Cell line 4	SYT-SSX2 (Synovial sarcoma)	SS18-SSX2 (Ex9/Ex6)	114/65%	2.10M/97%	298K/97%	73%	137bp	Pos	NA	NA
Clinical Case 1	EWS-WT1 (Desmoplastic small round cell tumor)	EWS-WT1 (Ex7/Ex7)	133/100%	2.05M/90%	73K/58%	81%	140bp	Pos	Pos	Pos (Ex7/Ex7)
Clinical case 2	EWS-FLI-1 (Ewing Sarcoma)	EWS-ERG (Ex7/Ex9)	124/100%	1.75M/95%	273K/30%	46%	170bp	Pos (Ex7/FLI1Ex9)	NA	NA
Clinical case 3	EWS-WT1 (Desmoplastic small round cell tumor)	EWS-WT1 (Ex7/Ex7)	33/100%	2.7M/79%	75K/36%	76%	131bp	NA	NA	Pos (Ex7/Ex7)
Clinical case 4	ASPL-TFE3 (Alveolar soft part sarcoma)	ASPL-TFE3 (Ex7/Ex6)	38/48%	2.5M/95%	96K/39%	79%	130	Neg	Pos	Neg*
Clinical case 5	NAB2-STAT6 (Solitary fibrous tumor)	NAB2-STAT6 (Ex2/Ex2)	1590/70%	1.8M/92%	46K/49%	77%	145	NA	NA	NA
Clinical case 6	EWS-NR4A3 (Extraskeletal myxoid chondrosarcoma)	TAF15-NR4A3 (Ex6/Ex3)	151/100%	2.56M/90%	100K/46%	80%	135	NA	NA	Neg*
Clinical case 7	EWS-FLI-1 (Ewing Sarcoma)	EWS-FLI-1 (Ex7/Ex6)	110/100%	2.39M/93%	102K/46%	78%	127	Pos (Ex7/Ex6)	NA	NA
Archer Control	EWS-FLI-1 (Ewing Sarcoma)	EWS-FLI- (Ex7/Ex6)	118/100%	2.25M/96%	236K/40%	53%	172bp	NA	NA	NA
NTC	NA	NA	0	0	0	0	0	NA	NA	NA

MBC= Molecular bar code; K= thousand, M= Million, bp= base pair, NTC= No template control.*Standard next generation sequencing gene panel does not include the gene partners involved in this translocation.

All cell lines and clinical samples (n=11; 100%) were positive for the expected translocations. The average total number of reads per sample was 1.8 million with an average total unique fragments RNA reads of 63.5 thousand (42% of total unique fragment reads). The average proportion of on-target RNA reads was 63%. Two cases that tested negative by NGS platform showed the expected translocations (ASPL-TFE3, TAF15-NR4A3) by RNA sequencing.
Conclusions: Our preliminary findings suggest that RNA based next generation sequencing is an efficient method for translocation detection in TA sarcomas. Limitations include RNA quality extracted from FFPE tissue. Additional testing is needed to further validate our findings.

2073 Utilization of Tumor Cell Enriched Cell Transfer Technique for Molecular Testing on H&E Stained Section of Small Biopsies in Comparison With the Routine Methods

Stephen Jovonovich, Liang Cheng, Melissa Randolph, Kristin Post, Joyashree Sen, Kendra Curless, Howard Wu. Indiana School of Medicine, Indianapolis, IN.
Background: Performing timely molecular testing for EGFR, BRAF, and KRAS mutations on certain newly diagnosed cancers has become the standard of care. The tumor cell enriched cell transfer technique (CTT) is potentially a viable option to obtain tumor cell DNA from H&E stained sections when the tissue is exhausted or only scant tumor cells remain within the paraffin block.
Design: This prospective study was performed during a period of 6 months between January 2014 and July 2014. Cell transfer technique was compared with the routine identification method for EGFR, KRAS or BRAF mutations on patients with a cancer diagnosis. Upon request, the histology departments took the paraffin block and cut 2 H&E stained slides (with 2 sections per slide) for the cell transfer method, and 4 unstained slides and one H&E stained slide for the routine method to extract tumor cells. The same panel of molecular tests was performed on material retrieved by the routine method one day and then on material retrieved by the cell transfer method the following day.
Results: The PCR-based molecular testing was successfully performed on 51of 63 (81%) CTT samples (20/27 cases for EGFR, 8/9 cases for BRAF, and 23/27 cases for KRAS mutations). Fifty of 51(98%) CTT samples showed correlation with the routine method, including 2 mutations and 18 wild types for EGFR, 2 mutations and 6 wild types for BRAF, and 8 mutation and 15 wild types for KRAS. There is one discrepancy being a CTT false negative KRAS (WT vs. G12C).
Conclusions: CTT performed on the original H&E stained cut sections is a viable tumor cell collection option for DNA molecular testing when the paraffin block tissues are exhausted or the tumor cells are scant on the recut sections. There is 98% agreement of the molecular testing results for CTT in comparison with the routine method.

2074 A Novel Tissue Array Technique Employing a Carrier Medium

Achim Jungbluth, Frosina Denise. Memorial Sloan Kettering Cancer Center, New York, NY.
Background: Blocks containing multiple tissues serving as test or control tissues for IHC and/or mloecular analyses have become important tools in surgical pathology. Depending on size and number of tissues, they are referred to as Multi-Tissue-Blocks (MTBs) or Tissue-Micro-Arrays (TMAs). While MTBs contain several larger tissue pieces, TMAs consist of up to several hundred tissue cores of usually <1mm.
However, in MTBs, the number of tissues is limited due to the size of the single

specimens and in TMAs, tissue cores are inserted into a plain paraffin block, often leading to signficant tissue loss due to trimming and/or loss of cores during the sectioning process.
We developed a method to optimize the generation of MTBs and TMAs by using an acceptor medium to ensure proper embedding of tissues and increasing the quality and number of sections which can be generated.
Design: We used circular dermatological punch devices in various diameters. A larger size was used to generate an acceptor tissue. This circular tissue was re-embedded and punches of smaller diameters were used to extract tissue cores, which were then filled with tissue cylinders of similar size from donor blocks. The new MTB consisting of acceptor tissue including the inserted tissue cylinders was re-embedded by melting the paraffin, then pushing all tissues in one level.
The same technique was used for TMAs: Instead of a plain paraffin, a carrier tissue/medium was used and the donor cores were inserted into the acceptor tissue/medium.
Results: MTBs of various sizes were constructed: for example an acceptor tissue of 12mm dimater with up to 9 tissue cores of 2-3mm. Similarly, TMAs were constructed by inserting tissue micro cores into an acceptor tissue instead of a plain paraffin block. Both, MTBs and TMAs were then re-embedded including melting paraffin and bringing acceptor and inserted tissue in one level. This was possible since the cores were kept in place by the scaffolding carrier tissue. The final block could be sectioned without major trimming resulting in optimal tissue use; moreover, no cores were lost as a result of sectioning and transfer to the slide. As carrier tissues, spleen, kidney and liver were best suited.
Conclusions: Generation of MTBs and TMAs is vastly improved by employing carrier tissues. They serve as scaffolding for the inserted tissues allowing proper re-embedding of a newly generated block. Our technique singificantly improves the yield of sections which can be generated from TMAs and MTBs and minimizes the loss of tissue cores during sectioning and transfer to the slide.

2075 Identification of Genomic Signatures in Circulating Tumor Cells From Breast Cancer

Nisha Kanwar, Pingzhao Hu, Philippe Bedard, Mark Clemons, David McCready, Susan Done. University Health Network, Toronto, ON, Canada; University of Manitoba, Winnipeg, MB, Canada; Ottawa Hospital Cancer Center, Ottawa, ON, Canada.
Background: Levels of circulating tumor cells (CTCs) in blood have prognostic value in early and metastatic breast cancer. CTCs show varying degrees of concordance with biomarkers of primary tumors they originate from. This is indicative of heterogeneity and evolution of tumor cells as they acquire new functionality and differential responses to chemotherapy. Profiling of CTCs will help identify occult changes occurring in breast cancer cells that facilitate a preferential passage into circulation and beyond.
Design: CTCs and matched normal white blood cells were isolated using immunomagnetic enrichment and single-cell laser microdissection, from the blood of 17/40 breast cancer patients. Copy number analysis was performed with the Affymetrix Genome-Wide Human SNP 6.0 array using a paired tumor-normal approach. Minimal common regions (MCRs) of recurrent genomic gain were extrapolated, followed by unsupervised clustering. A TCGA copy number dataset of 787 primary invasive breast tumors was queried for CTC-like alterations.
Results: We identified a signature of recurrent gain in CTCs, consisting of 90 MCRs. These were predominantly found across chromosome 19 and were identified at low frequencies (3-4%) in 787 primary tumors examined. CTC genomic profiles clustered into 2 groups independent of subtype: a dormancy-related signature with 15 MCRs (AKT2, PTEN, CADM2); and a tumor-aggressiveness signature with 398 MCRs, of which 54 were on chromosome 19 (ANGPTL4, BSG, MIR-373). There were 2 MCRs in common between the groups on 19p13 and 21q21, containing genes involved in resistance to anoikis, TGFβ signaling, and metastasis (TFF3, LTBP4, NUMBL). A 1.2Mb amplicon containing the ERBB2 gene was gained in 15/17 patients, irrespective of the HER2 status of the primary tumors. Regions 20q13 and 15q24 were associated with distant metastasis.
Conclusions: CTCs appear to be more homogeneous for certain genomic gains, specifically on chromosome 19. The distinctiveness of CTC signatures highlights cell populations with different functional or metastatic potential. We are using multi-spectral FISH to detect the proportion of cells within primary tumors with CTC-like signatures. Such novel targets could help to specifically identify and block dissemination.

2076 A Molecular Pap Test – Using Raman Spectroscopy for Detection of High Grade Cervical Neoplasia in Exfoliated Cervical Cells

Padraig Kearney, Damien Traynor, Franck Bonnier, Fiona Lyng, Cara Martin, John O'Leary. Trinity College and Coombe Womens and Infants University Hospital, Dublin, Ireland; Focas Institute, Dublin Institute of Technology, Dublin, Ireland.
Background: Cervical screening for detection of cervical intraepithelial neoplasia is very effective in reducing the incidence of cervical cancer. Current screening protocols use the Pap test, but this can be subjective and can often exhibit low specificity and sensitivity. For this reason, improved methods for cervical screening are required to improve performance of cervical cancer screening methods, particularly in the context of vaccinated cohorts. Raman spectroscopy is a powerful tool that can generate a biochemical fingerprint of a sample in a rapid and non-destructive manner.
Design: In this study, Raman spectroscopy has been applied to discriminate between different cervical cell types in PreservCyt cervical smear specimens. Raman measurements were taken from the nuclei of 50 normal cells and 50 HSIL cells. These spectra were processed, analysed and used to define/classify a spectral signature for high grade cervical disease. Principal Component Analysis (PCA) was used to discriminate between the two data sets.
Results: Distinct Raman spectral differences were detected between normal cervical cell types and HSIL cells. In CIN3 spectra, it is possible to observe spectral peak shifts representing Guanine (DNA/RNA), CH deformation in proteins and carbohydrates, Tryptophan, Carbon-carbon double bonds in Phenylalanine, Tyrosine and Tryptophan, and Amide I. These protein expression and nuclear changes reflect the difference between the mature superficial cells and the highly proliferative CIN3 cells. The PCA showed an excellent discrimination between the data sets, with all but one spectra being correctly classified.
Conclusions: Raman spectroscopy is a very powerful tool which can detect subtle changes between cervical cells, and may be useful for improved diagnosis of cervical dysplasia.

2077 Margin Assessment of Breast Lumpectomy Specimens: Perpendicular Margins Effectively Establish Margin Status Resulting in Lower Utilization of Laboratory Resources

Michael Keeney, Judy Boughey, Elizabeth Habermann, Amy Wagie, Daniel Visscher, Gary Keeney. Mayo Clinic, Rochester, MN.
Background: In breast conserving surgery (BCS) for breast cancer, the method of margin assessment varies widely, often impacting laboratory workload and costs. Some advocate for the use of shave margins (SM) rather than perpendicular sections (PS) as a means of conducting a more complete margin analysis. Although the SM method is widely used, little is known regarding the clinical utility of this method compared to the PS method. The purpose of this study was: 1) to compare the incidence of positive margins and rates of intraoperative reexcision between the SM and PS margin assessment methods, and 2) to assess the number of slides for each method in the setting of the three most common breast cancer diagnoses – ductal carcinoma in situ (DCIS), invasive ductal carcinoma (IDC), and invasive lobular/mixed carcinoma (IMC).
Design: From 4/2012-10/2013, 513 patients underwent BCS at our institution, including 423 diagnosed with DCIS, IDC or IMC. Of these, 394 cases had residual tumor for analysis. The effect of the method of margin assessment on positive margin rate and total block count per case was evaluated using chi-squared and t-tests for tumor type and intraoperative margin status.
Results: Of the 394 cases, 253 (64%) had a reported positive intraoperative margin. When considering the diagnoses of DCIS, IDC and IMC together, the SM and PS methods were equally effective at identifying the positive margin (35% versus 36%, p=0.8089); however, SM required nearly three times the block count per case (28 versus 10, p<0.0001) and was more commonly utilized in cases with DCIS than invasive disease (75% vs 60%, p=0.0139) compared to PS. Analyses stratified by diagnosis (DCIS, IDC, IMC) showed similar rates of positive margin identification for SM and PS in each of the 3 cancer types (Figure 1).
Conclusions: Our data suggest that the SM and PS methods are equally effective at identifying positive margins in three distinct categories of breast carcinoma. The SM method of margin assessment significantly increases the total block count and therefore the allocated resources per case without adding any clear diagnostic benefit. Clinical follow-up is needed to determine whether long-term benefits for either method exist.

Figure 1

		Negative	Positive	Total	P-Value
		141	253	394	0.8089
Overall	Perpendicular	91 (65.0%)	49 (35.0%)	140	
	Shave	162(63.8%)	92 (36.2%)	254	
		Negative	Positive	Total	P-Value
		29	84	113	0.3654
DCIS	Perpendicular	9 (32.1%)	19 (67.9%)	28	
	Shave	20 (23.5%)	65 (76.5%)	85	
		Negative	Positive	Total	P-Value
		101	137	238	0.2664
IDC	Perpendicular	37 (38.1%)	60 (61.9%)	97	
	Shave	64 (45.4%)	77 (54.6%)	141	
		Negative	Positive	Total	P-Value
		11	32	43	0.719
IMC	Perpendicular	3 (20.0%)	12 (80.0%)	15	
	Shave	8 (28.6%)	20 (71.4%)	28	

2078 A High Mutation Frequency Allows for Detection of Endometrial Cancer in Brush Cytology Specimens By Next Generation Sequencing

Sarah Kerr, Jesse Voss, Chen Wang, Karl Podratz, Trynda Kroneman, Emily Barr Fritcher, Kevin Halling, Jamie Bakkum-Gamez, Benjamin Kipp. Mayo Clinic, Rochester, MN.
Background: Endometrial cancer (EC) is a curable disease in early stage, but EC mortality has far surpassed uterine cervical cancer since implementation of Pap test screening. Clinical uptake of endometrial brush cytology (EBC) screening for EC has been slow due to perceived challenges in morphologic interpretation. Extensive molecular analysis of EC has shown frequent mutations in a limited number of genes. Next generation sequencing (NGS) provides the opportunity to exploit these mutations for cancer detection, and offers the potential of a sensitive, specific, and cost-effective screening test.
Design: A targeted NGS assay using custom PCR amplification primers followed by orthogonal Illumina® and Ion Torrent™ sequencing chemistry was designed to cover 19 genes frequently mutated in EC, including the full coding region of tumor suppressors *PTEN*, *TP53*, *FBXW7*, *ARID1A*, *PIK3R1*, *CDKN2A*, and *POLE*, and targeted regions of oncogenes *PIK3CA*, *KRAS*, *FGFR2*, and *CTNNB1*. Copy number variation (CNV) detection was also bioinformatically possible for some amplicons. Mutation or CNV

detection was considered a positive test result. DNA was extracted from EC tumor positive (TP) and tumor negative (TN) cell pellets derived from EBC specimens collected prior to hysterectomy (diagnostic gold standard).
Results: Selected cell pellets consisted of 19 TP and 9 TN cases. TP cases represented 10, 3, and 3 endometrioid grade 1, 2, and 3 ECs, respectively; 2 clear cell ECs; and 1 mixed endometrioid and clear cell EC. Fifty-three mutations were detected in 13 genes and 15 of 19 TP samples. Mutations detected per TP sample ranged from 0 to 10 (mean 2.7, median 2). Mutant allele frequencies ranged from 5 to 61% (mean 21%). CNV was detected in 10 of 19 TP samples for a final detection rate of 16 of 19 TP cases using both mutation and CNV data. No mutations or CNVs were detected in the 9 TN samples, providing assay sensitivity and specificity of 84% and 100%. All 3 false negative samples represented grade 1 or 2 endometrioid ECs.
Conclusions: This pilot project demonstrates the feasibility of using NGS for detection of EC in EBC specimens. Lower grade ECs may be more difficult to detect due to lower tumor burden, mutation rates and/or copy number variation. Further studies are needed to determine the best cost-effective screening approach to reduce the morbidity and mortality in women from EC.

2079 Feasibility of Using Ex-Vivo Full Field Optical Coherence Tomography for Immediate Assessment of Tumor Cellularity in Image Guided Core Needle Biopsies

Savitri Krishnamurthy, Andrea Cortes, Sharjeel Sabir, Michael Riben, Stanley Hamilton, Kenna Shaw, Gordon Mills, Michael Wallace. University of Texas MD Anderson Cancer Center, Houston, TX.
Background: Procurement of high-quality core needle biopsy samples (CNBs) is critical for enabling diagnosis and performance of ancillary molecular testing for targeted therapies. In this prospective study, we investigated the feasibility of a full-field OCT (FF-OCT) platform for immediate assessment of tumor cellularity in CNBs procured by interventional radiology.
Design: A single image-guided 18- or 20- gauge CNB was imaged at 20 µm beneath tissue surface using a Light-CT scanner. Hematoxylin-eosin-stained tissue sections of the CNBs were prepared for histopathology (HP). Based on the HP, the CNBs were categorized in three groups: no tumor/fibrosis/normal tissue, <25% tumor cellularity, and ³25% tumor cellularity corresponding to the minimum tumor content required for next generation sequencing. The tumor cellularity in the FF-OCT images was compared with the estimation made from HP and the extent of agreement was evaluated with kappa statistic.
Results: We successfully imaged 35 of 46 CNBs obtained from different sites (lung-13, liver-8, lymph nodes (LN)-11, soft tissues-3). HP showed no evidence of tumor in 12 (34%) of the 35 CNBs (lung 4/13, liver 2/8, LN 6/11), tumor cellularity < 25% in 8 (23%) CNBs (lung 5/13, liver 1/8, LN 2/11), and tumor cellularity ≥ 25% in 15 (43%) CNBs (lung 4/13, liver 5/8, LN 3/11, soft tissues 3/3. Tumor cellularity findings in optical images of the CNBs matched with HP in 7(58%) of the 12 CNBs with no tumor (lung 1/4, liver 0/2, LN 6/6), 5 (63%) of the 8 CNBs with <25% tumor cellularity (lung 4/4, liver 0/2, LN 1/2), and all 15 CNBs with ³25% tumor cellularity. Overall, tumor cellularity was overestimated in optical images in comparison with HP with the coefficient of agreement between the two methods of 0.66; 95% confidence interval 0.45–0.87.
Conclusions: 1. All 15 CNBs with ³25% tumor cellularity were correctly categorized on FF-OCT images irrespective of biopsy site. 2. Overestimation of tumor cellularity in optical images occurred in CNBs with no tumor or <25% tumor cellularity and resulted from the inability of the optical method to distinguish tumors from stromal fibrosis, inflammation, and non-neoplastic tissue. 3. FF-OCT is a promising modality for immediate assessment of CNBs for sequencing, but improvements are warranted for better distinction of tumors from fibrosis/non-neoplastic tissue.

2080 Phospho-Histone H3 Stain Increases Inter-Observer Reproducibility and Is More Efficient Than H&E Stain To Evaluate Mitotic Index in Breast Cancer

Xiaoxian Li, Stephen Wells, Guilherme Cantuaria, Vaishali Pannu, Nikita Wright, Sergey Klimov, Padmashree Rida, Ritu Aneja, Michelle Reid. Emory University Hospital, Atlanta, GA; Northside Hospital Cancer Institute, Atlanta, GA; Georgia State University, Atlanta, GA.
Background: Mitotic index (MI) is a useful prognostic indicator for breast cancers. MI is routinely determined via visual recognition of mitotic figures, which can be time consuming and objective. While visual distinction between apoptotic cells from mitotic cells (both with condensed DNA) is prone to subjectivity, it is also challenging to recognize mitotic phases, prophase, in particular. Phospho-histone H3 (PH3) has been shown to be a specific mitotic marker. Here we evaluated the MI from 42 cases stained with PH3 and H&E and compared their inter-observer reproducibility and efficiency in practice.
Design: Pre-marked tumor areas were blindly scored for MI in 10 high power field by 3 pathologists using H&E or PH3 staining. We used the Intraclass correlation coefficient (ICC) to assess the consistency of measurements made by the 3 pathologists. Time taken to score each H&E and its paired PH3-stained counterpart was also recorded.
Results: We found that a) there was a moderate positive correlation between MI using H&E and PH3 stain ($r=0.35$, $p<0.001$); b) there was a significant increase in agreement among the 3 pathologists when evaluating MI using PH3 staining (ICC=0.57) as compared to MI using H&E staining (ICC=0.38) ($p<0.05$); c) PH3 staining was more efficient in identification of mitotic cells. Time taken by each pathologist in scoring PH3 slides was 25-50% lower than H&E slides, irrespective of the individual scoring time differences between the 3 pathologists.
Conclusions: PH3 stain significantly increases inter-observer reproducibility than H&E stain in evaluation of MI. PH3 stain is more efficient than H&E stain in identification of mitotic activity in breast cancers.

2081 Impact of Tissue Decalcification on Immunohistochemical Detection of Select Markers for Carcinoma of Unknown Origin

Fan Lin, Jianhui Shi, Zongming Chen, Haiyan Liu. Geisinger Medical Center, Danville, PA.
Background: Application of an immunohistochemical (IHC) assay on decalcified tissues is frequently performed in an anatomic pathology laboratory. It has been documented that tissue decalcification (decal) may have a negative impact on an assay for certain antigens. In this study, we investigated the impact of decal on the detection of commonly used markers for carcinoma of unknown origin using cultured cancer cell lines.
Design: Seven cancer cell lines from various organs (lung, breast, pancreas, thyroid, colon, kidney and uterine cervix) were obtained from the American Type Culture Collection. A set of IHC markers was tested on each cell line on a cell block. These 7 cell lines collectively expressed the following target markers: CK7, CK20, CK5/6, p40, p63, TTF1, CDX2, SATB2, PAX8, ER, PR, GATA3, GCDFP15, CD56, synaptophysin, chromogranin, calcitonin, MUC1, MUC2, CEA, BerEP4, maspin, S100P, IMP3, beta-catenin, p16, P504S, vimentin, and HPV in situ hybridization. The cell pellets containing a mixture of the 7 cell lines were first fixed in 10% neutral buffered formalin for 8 hours (h) and then decalcified in Decalcifier B (Fisher Healthcare, item #23245683) for the following durations: 0 minutes (min) (no decal), 30 min, 60 min, 3 h, 6 h, 1 day, 3 days and 1 week. A tissue microarray (TMA) block containing these tissue/cell line cores with the different decal times was constructed. The aforementioned IHC markers were applied to the TMA sections using the Ventana Ultra staining platform. The staining intensity was recorded as strong (S), intermediate (I), or weak (W). The percentage of cells stained was recorded as 0, 1+, 2+, 3+, or 4+ and compared to the sample with no decal.
Results: Tissue decal has little impact on the detection of CDX2, PR, chromogranin, calcitonin, BerEP4, S100P, GCDFP15, p16, P504S, vimentin, CK7, CK20, CK5/6, and CD56 after 1 week's decal. The impact of decal on other tested IHC markers is summarized in the table below.

Time of Decalcification	Significant negative impact on tested IHC markers
Any time in decalcification	HPV in situ hybridization
After 60 minutes	SATB2, PAX8, GATA3, ER, maspin, IMP3, p40, p63
After 3 hours	TTF1
After 1 day	Synaptophysin, MUC1, MUC2, beta-catenin
After 3 days	CEA

Conclusions: These data demonstrate that tissue decal has various impacts on antigen detection. These data can serve as a reference for these particular markers. Caution should be taken when performing an IHC assay on decalcified tissues.

2082 BRAF V600E Mutation in Melanoma, Colorectal Carcinoma, Hairy Cell Leukemia, Papillary Thyroid Carcinoma, and Langerhans Cell Histiocytosis: Concordance Between Molecular Testing and Mutation-Specific Immunohistochemistry

Eric Loo, Parisa Khalili, Karen Buehler, Imran Siddiqi, Mohammad Vasef. University of New Mexico, TriCore Laboratories, Albuquerque, NM; TriCore Reference Laboratories, Albuquerque, NM; University of Southern California, Los Angeles, CA.
Background: The *BRAF* V600E mutation has been identified in melanoma, colorectal carcinoma (CRC), papillary thyroid cancer (PTC), hairy cell leukemia (HCL), and Langerhans cell histiocytosis (LCH). Patients with *BRAF* mutated metastatic melanoma show dramatic response to BRAF inhibitors. Other *BRAF*-mutated tumors may also benefit from BRAF inhibitors. Currently, *BRAF* mutational testing is performed by molecular methods in most laboratories. However, recently a mutation-specific antibody (MSA) has become available. Studies to validate correlation between the molecular and IHC methods are sparse. We validated the *BRAF* V600E MSA on several different tumors and correlated the results with the molecularly determined *BRAF* mutational status.
Design: A total of 69 cases with prior molecular testing for *BRAF* mutation by pyrosequencing or next generation sequencing were pulled for IHC. The cases included 19 CRC, 21 melanoma, 10 PTC, 11 LCH, and 8 HCL. IHC was performed on recuts of diagnostic blocks using a *BRAF* V600E MSA.
Results: All 32 cases with molecularly characterized *BRAF* V600E mutation were positive with V600E MSA indicating complete concordance. 34 *BRAF* wild type and 3 variant *BRAF* V600K mutated cases were negative with V600E MSA, consistent with high specificity of the antibody. The staining pattern was cytoplasmic and membranous with moderate to strong intensity. However, 4 out of 6 bone marrow biopsies with HCL that had been fixed in acetic acid zinc formalin showed weak intensity. The staining in 2 remaining formalin-fixed HCL cases showed moderate to strong intensity.

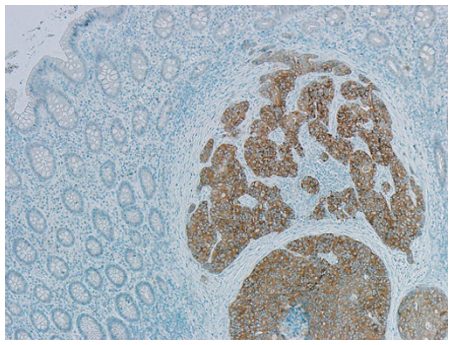

Conclusions: The *BRAF* V600E MSA appears to be clinically useful in assessing *BRAF* V600E mutation status with high degree of sensitivity and specificity. We see a high degree of concordance between *BRAF* testing by IHC and molecular methods. Immunohistochemistry is a more cost effective alternative compared to molecular testing with a shorter turn-around-time for *BRAF* testing.

2083 Triple Negative Breast Cancers Evaluated By Amplified mRNA In-Situ Hybridization for Estrogen Receptor-Alpha

Krishnan Mahadevan, Atul Bhan, Vikram Deshpande, Elena Brachtel. Massachusetts General Hospital, Boston, MA.

Background: Triple negative breast cancers do not express estrogen receptor (ER), progesterone (PR) or HER2, and comprise a subset with unfavorable prognosis. ER may be difficult to quantitate in cases of low protein expression. Since even faint staining may allow hormonal therapy, the distinction between ER+ and ER- is of high clinical importance but can be hampered by relatively low interobserver agreement in cases with low or absent ER protein. In this study, we used a novel amplified mRNA in-situ hybridization technique to demonstrate ER transcripts in human breast cancers and correlate the findings with ER protein expression.

Design: Sixty-seven ER-PR-HER2- invasive ductal carcinoma tissue samples from female patients with a mean (median) age of 59 (63) years and tumor size of 2.7 cm (range 0.7-11 cm) were selected and tissue microarrays constructed. 45 samples were from ER+ breast cancers. Immunohistochemistry was performed with ER clone 6F11, PR 16 and HER2 4B with Leica Bond autostainer and reported according to national guidelines. In-situ hybridization (ISH) was performed with ER-alpha probe ER-VA012 (QuantiGene®) and ViewRNA Technology (Manual 1-Plex Assay kit, Affymetrix, Santa Clara, CA) after deparaffinization, tissue fixation and pre-treatment. The probe signal was amplified with complementary zDNA, visualized with fast red substrate and counterstained. The TMAs were manually scored as positive if >10 signals/cell were present.

Results: 61 of 61 ER- cases showed low number of ER transcripts by ISH with concordant results in 100% (tissue loss in 6 cases). Strong ER protein expression correlated with abundant ER mRNA signals. Low number of ER signals (<10/cell) was seen in 4 cases with faint ER protein expression. Examples: IDC H&E (A) ER+ by IHC (B) and high number of ER signals by ISH (C). IDC H&E (D) ER- by IHC (E) and low number of ER signals by ISH (F).

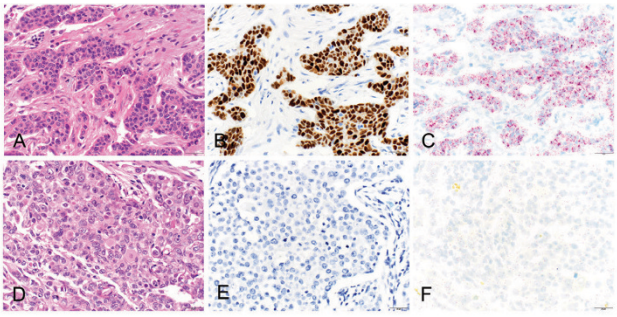

Conclusions: The excellent concordance of ER mRNA levels with ER protein expression as demonstrated in this study may permit more accurate ER determination in breast cancers with faint ER protein expression. In contrast to other molecular methods, in-situ hybridization allows visualization of RNA transcripts with preserved tissue integrity.

2084 Effect of Storage Time of FFPE Ovarian Cancer Tissue on DNA Quality for Next Generation Sequencing

Hala Makhlouf, Irina Lubensky, Sean Altekruse, Michele Mehaffey, Michael Sachs, Corinne Camalier, Rodrigo Chuaqui, Wendy Cozen, Das Biswajit, Brenda Hernandez, Chih-Jian Lih, Charles Lynch, Paul McGregor, Lisa McShane, JoyAnn Philips Rohan, William Walsh, Mickey Williams, Elizabeth Gillanders, Leah Mechanic, Sheri Schully, Danielle Carrick. National Cancer Institute, Rockville, MD; Leidos, Frederick, MD; University of Southern California, Los Angeles, CA; University of Hawaii Cancer Center, Honolulu, HI; University of Iowa, Iowa City, IA.

Background: Next Generation Sequencing (NGS) technique is becoming important in cancer care as the era of targeted medicine rapidly evolves. FFPE tissue has been the most commonly available clinical specimen for solid tumors histopathology, thus there is a need to determine whether long-term stored FFPE specimens can be reliably utilized for sequencing in large-scale clinical and population studies.

Design: 59 FFPE high grade ovarian serous adenocarcinomas (HGOSC) stored between 3 and 32 years were obtained from 3 Residual Tissue Repositories (RTR) linked to the NCI Surveillance, Epidemiology and End Results (SEER) registries. DNA was extracted using the Qiagen FFPE tissue kit and subjected to whole exome sequencing (WES) on a HiSeq2000 using Agilent Sure. Consistency with the tissue selection criteria was determined by pathology re-review (i.e., HGOSC had ≥50% cells with tumor nuclei and <50% necrotic cells).

Results: DNA quantity and quality were significantly associated with storage time. 58/59 specimens (98%) yielded sufficient DNA (>50ng) for subsequent generation of library preps followed by WES. Overall, 90% (53/59) of specimens provided successful WES data regardless of storage time (table1). Analysis of the DNA yields and quality by SEER registry site did not show statistically significant differences.

	Mean (SD) by Storage time				Difference (95% CI),10 y of Storage time	P-value
	Overall N=53	3-12 Y N=12	13-22 Y N=29	23-32 YN=12		
Final Library Size (bp)	275.3 (11.3)	277.2 (6.7)	277.6 (12.1)	267.9 (10.3)	-8.5 (-13.4 to -3.5)	P = 0.001
% Target Covered 20x	86.2 (7.9)	89.7 (2.8)	86.3 (8.3)	82.2 (9)	-6.1 (-9.5 to -2.6)	P
Avg Read Depth	112.1 (48.4)	128.2 (35.5)	116 (51)	86.8 (46.8)	-39.1 (-60 to -18.2)	P
% Duplication	33.6 (20.9)	26.6 (13.9)	34.1 (21.5)	39.5 24.5)	9 (-0.9 to 18.8)	P = 0.074
Ti/Tv Ratio	2.48 (0.15)	2.43 (.07)	2.45 (.08)	2.61 (0.24)	0.12 (.06 to 0.18)	P

Conclusions: This study demonstrates that FFPE specimens acquired from SEER registries stored for different lengths of time and under varying storage conditions are a good source of DNA for NGS.

2085 In Situ Imaging and Quantitation of a Flow-Cytometric Phenotype (CD4+/CD25+/FOXP3+) for Regulatory T Cells in Squamous Cell Carcinoma FFPE Sections

James Mansfield, Christian Slater, Kenneth Oguejiofor, Richard Byers. PerkinElmer, Hopkinton, MA; University of Manchester, Manchester, United Kingdom.

Background: Cancer immunotherapy is rapidly changing the landscape of cancer treatment, and monitoring the immune status of a patient is a critical aspect of research in this field. One particular area of interest in immuno-oncology is the role of regulatory T cells (Tregs). Beginning with the discovery of CD4+/CD25+/FOXP3+ Tregs in 1995, the list of Treg subsets and their function in tumors and other tissues has grown considerably. While quantifying specific subsets of immune cells is routine using multimarker flow cytometry, monitoring the numbers and distribution of these same subsets of immune cells in FFPE biopsies of solid tumors remains unobtainable with standard methods. To address this we present here a methodology for staining, imaging and analyzing the CD4+/CD25+/FOXP3+ phenotype of Tregs in head and neck squamous cell carcinoma (HNSCC) FFPE specimens.

Design: A sequential multiplex staining using tyramide signal amplification (TSA) conjugated fluorophores with DAPI nuclear counterstain. Imaging was performed using a multispectral imaging system, which enabled the quantitative separation of the fluorophores and elimination of autofluorescence. Image analysis was executed using an automated image analysis program. Each 20x image underwent a morphologic segmentation into tumor, stromal and blank regions. The CD4+/CD25+/FOXP3+ phenotype cells were identified using a new multinomial logistic regression which uses features derived from unmixed images, texture analysis and cell segmentation, and then enumerated in the tumor and in the stroma of the sample.

Results: Developing a staining, imaging and analysis protocol for CD4+/CD25+/FOXP3+ Tregs was relatively straight forward. Cells with this particular triple-marker phenotype were identified and differentiated from other non-triple-positive cells. The counts obtained from the automated analysis correlate well with human visual assessment of the images.

Conclusions: The automated assessment of the Treg phenotype correlates well with the visual assessment. As each cell needed to be checked to see whether it expressed all three of the markers this was an extremely laborious process. However, this study shows the utility of automating the assessment of a flow-cytometric phenotype for Tregs *in situ* in FFPE tissue sections. This methodology can be expanded to 7 or 8 markers to give for the first time a truly "tissue cytometric" analysis.

2086 Validation and Clinical Correlation of Triplex CD3, CD8 and FOXP3 IHC of Tumor-Infiltrating Lymphocytes in Follicular Lymphoma

James Mansfield, Christian Slater, Kenneth Oguejiofor, John Hall, Richard Byers. PerkinElmer, Hopkinton, MA; University of Manchester, Manchester, United Kingdom.

Background: It is becoming apparent that immune cells play conflicting roles within the tumor microenvironment. As such there is increasing demand for methodologies that would allow for the analysis of the distributions of accurately phenotyped immune cells in-situ in solid tumors. Existing methods can either deliver phenotypic information on homogenous samples (e.g., flow cytometry) or morphologic information limited to cells positive for single immunomarkers (standard IHC). These limitations can be largely overcome through multiplexed staining, multispectral imaging and analysis methodology. Although multiplex methods have been shown to be particularly useful statistical validation remains scarce. We present a validation of such a method for CD3, CD8 and FOXP3 in follicular lymphoma.

Design: A tissue microarray containing triplex follicular lymphoma cores from 40 subjects [24 male, 16 female, age 35 to 75 years at diagnosis, median 55 years, 2- 171 months follow-up] was used. Multiplex IHC involved a sequential multi-marker labeling technique for 3 antigens and a counterstain. Automated multispectral imaging was used to separate chromogens and automated image analysis was used to quantitate the per-cell marker expression, determine the cellular phenotype, and count these cells separately in the tumor compartment and in the stroma. Results from the triplexed method were compared directly to those obtained from adjacent singly stained sections. Spearman rank correlation (non-parametric) was used to study the concordance of per-cell quantitation for the three biomarkers individually in single stained sections compared to adjacent multiplex stained sections. Chi squared test was used to compare groups for statistical differences.

Results: Spearman rank correlation showed a good agreement (R^2>0.9; P<0.0001 in all cases) and Chi squared test demonstrated no statistically significant difference (P>0.05) between scores obtained from multiple-stained sections compared to single stained sections, suggesting that multiplexed staining methods can replicate standard IHC methods while maintaining the inter-distribution and visualization of the markers in a single section.

Conclusions: The understanding of the inter-distribution of multiple subsets of immune cells in tumors is important in cancer, and only multiplexed IHC offers the possibility to image and quantify these distributions. This study shows it is possible to replicate singleplex scoring and cell counting in a multiplexed IHC context with a high degree of confidence.

2087 Fluorescent Sorting and Printing of Single Cells in Cancer Applications

Victoria McEneaney, Helen Keegan, Michael Gallagher, Andre Gross, Cara Martin, Orla Sheils, Peter Koltay, John O'Leary. Trinity College, Dublin, Ireland; IMTEK, Freiburg, Germany.

Background: The EU Framework 7 project (PASCA: Platform for Advanced Single Cell Manipulation and Analysis) has developed a novel instrument referred to as a Single Cell Printer (SCP) which enables 1) rapid optical and fluorescent detection of single cells 2) generation of picoliter sized droplets encapsulating the isolated single cell and 3) printing of the single cell in an "ink-jet" like manner onto a chosen substrate. This technology was used to isolate cells of interest from heterogeneous mixed populations of cells, co-cultures of cells and clinical patient samples.

Design: The piezo driven "drop - on - demand" system contains a robotic dispensing unit coupled to a micro dispenser chip. The chip contains micro fluidic structures that guide the cell suspension with an actuator deflecting onto a membrane, thus dispelling a single droplet. A detection algorithm monitoring the chips exit nozzle selects single cells for dispensation whilst a pneumatic shutter system removes unwanted droplets in flight, thus ensuring only droplets containing a single cell are printed. Other key features allow monitoring of droplet size, shape and velocity by an embedded stroboscopic camera whilst a substrate camera allows verification and visualisation of printing efficiency.

Results: The SCP technology has been applied (but is not limited) to cervical cytopathology, anaplastic thyroid carcinoma and cancer stem cell studies. In the cervical cytopathology application, Human papillomavirus (HPV) positive cells have been fluorescently isolated from HPV negative clinical cervical samples based on E7 protein detection. Printing of the isolated cells into spatially ordered arrays along a microscope slide are ongoing. In the anaplastic thyroid application, the SCP technology has been used to sort drug treated responsive cells from non responsive cells for biological analysis at a single cell level. In the cancer stem cell application, co cultures and mixed populations of cells were sorted based on surface expression markers indicative of differentiation status.

Conclusions: SCP technology may assist in analysis of individual cells within many tumours and from many disease types, thus leading to a greater understanding of the complexities within clinical diagnostics and therapeutics.

2088 Evaluation of Ki-67 (MIB-1) Labeling Index With Dual-Color Immunocytochemistry (Ki-67 with LCA) for Grading of Pancreatic Neuroendocrine Tumors

Linette Mejias, Amarpreet Bhalla, Nagla Salem, Sumi Thomas, Vinod Shidham. Wayne State University, Detroit, MI.

Background: Ki67 (MIB-1) immunohistochemistry to quantify the proliferative index (PI) of pancreatic neuroendocrine tumors (PanNET) has been recommended in the literature. However, this has a number of challenges due to interference by Ki67 immunostained lymphocytes infiltrating the tumor and also some cells in stroma including endothelial cells. There is lack of consistent recommendations to overcome this issue. Our pilot project showed that two color immunostaining with inclusion of LCA (Ki67 nuclear brown & LCA Cytoplasmic red) can facilitate the weeding out of lymphocyte interference to a large extent.

Design: We studied 21 cases of PanNET. All cases were categorized by using Hochwald et al. grading after counting mitotic figures in 50 high power fields (hpf) (7 Grade 1, 16 Grade 2).

Dual color immunostaining (Ki67 with LCA) (Method I) was performed on sections of representative blocks along with single color Ki-67 without LCA (Method II) on adjacent section. Ki67 index (KI) was calculated using single and dual color methods both manually and by digital method (Ventana Image-VIAS). Digital method overestimated the KI in both single and dual color immunostained sections and was not considered effective. For manual counting, 500 cells in areas with highest nuclear labeling but least number of LCA immunostained cells (in dual stained sections) were counted. Percent number of Ki67 immunoreactive cells calculated manually by two methods were compared using the Wilcoxon test for two related samples and correlated with grading.

Results: Grade1 PanNET: Average KI by method I was 1 (0 to 3) with an average of 3 (0 to 4) by method II (p value 0.038).

Grade2 PanNET: Average KI was 6 (0 to 31) by method I and 7 (2 to 40) by method II (p value 0.004).

The differences by two methods were statistically significant in both grade 1 and 2 with tendency for higher counts by single color (method II).

Conclusions: Dual-color immunostaining for Ki-67 with LCA estimated Ki67 with higher precision, due to ability to exclude LCA immunoreactivity infiltrating lymphocytes. Other non-tumor Ki67 immunoreactive cells such as some endothelial cells can be distinguished morphologically by both manual methods. Digital methods could not distinguish infiltrating lymphocytes and other cells in sections.

For precise grading of PanNET, routine application of dual color Ki67 immunostaining is recommended. This is critical for evaluation of small biopsies and cell block sections of FNA material.

2089 Multiplex Tissue and Clinical Proteomics By Next-Generation Sequencing

George Miles, Yongmei Zhao, Yelena Levin, Jyoti Shetty, Bao Tran, Stephen Mitchell, J Carl Oberholtzer, David Levens. National Cancer Institute, Bethesda, MD; Frederick National Laboratory, Frederick, MD; Holy Cross Hospital, Silver Spring, MD.

Background: The simultaneous measurement of many different proteins presents a major challenge to the fields of surgical and clinical pathology, and there is a genuine need for the development of a more direct, quantitative approach to multiplex analysis of proteins in tissues and clinical assays. Here we present a novel, high-throughput immunoassay, driven by the hypothesis that highly sensitive, multiplex protein characterization can be obtained by coupling the unique specificity of antibodies with massively parallel sequencing to detect and quantitate antigens from formalin-fixed, paraffin-embedded tissue (FFPE) and in solution.

Design: To profile the abundance of select targets in breast carcinoma, libraries of antibody-oligonucleotide heteroconjugates of defined stoichiometry were constructed for ER, PR, Her2, and EGFR. Each conjugate was tagged with a barcode of nucleotides providing metadata to the cognate antigen for the antibody as well as for each antibody molecule in the library. Breast carcinoma tissue arrays were incubated with mixtures of up to 8 different antibody libraries. Additionally, target antigens were evaluated in an ELISA-like assay. Following antibody binding in either case, the barcoded oligonucleotides were purified, amplified by PCR, and sequenced. The number of unique sequence identifiers was used to determine the relative amounts of each protein. Routine immunohistochemistry (IHC) and ELISAs were performed in parallel to sequencing experiments.

Results: Sequencing from all experiments yielded ~332 Gigabases of data, with over 6.4 billion pass-filter reads that were further refined to ~1.5 billion unique reads [mean Q score(PF)=37.4; Q30+ bases >92%]. We quantified eight antigens in 48 different patients in parallel (384 total targets) using FFPE specimens with a dynamic range approaching 7 logs. Correlation plots between tissue replicates were performed (r^2=0.99). The sequencing counts correlated with the visual intensity of staining by IHC. Further, we could detect and measure the amounts of single or multiple, pooled antigens in solution using an ELISA-like assay, detecting Her2 antigen at ~$1x10^{-4}$ pM.

Conclusions: We have extended the application of next generation sequencing to allow for the highly sensitive, multiplex detection and digital counting of proteins on fixed tissue and in solution. This technology may serve as a means for the quantitative investigation of functional genomics, and for diagnostic applications.

2090 Nanopore Sequencing of a DNA Library Prepared From Formalin-Fixed Paraffin-Embedded Tissue

George Miles, Jessica Hoisington-Lopez, Eric Duncavage. Washington University, St. Louis, MO.

Background: Nanopore sequencing has the potential to revolutionize molecular genetic testing through the direct and real-time analysis of DNA on a mobile platform that could potentially enable point of care molecular diagnostics. Currently little is known about the performance of nanopore sequencing in the clinical molecular oncology laboratory. We evaluated the performance of nanopore sequencing on target-enriched nucleic acids derived from routine formalin-fixed, paraffin embedded (FFPE) diagnostic specimens.

Design: DNA was extracted from routine FFPE surgical resection specimens and target enriched using a hybrid-capture panel targeting 151 genes commonly mutated in cancer. Following hairpin ligation and tether annealing, the modified libraries were loaded into a primed MinION flow cell. Read quality and sequencing metrics were evaluated using the included bioinformatic tools and sequences were mapped to the human genome (hg19) using discontiguous-megablast and the Burrows-Wheeler Aligner

(BWA); reads with mapped expect values $<10^{-4}$ were considered adequately mapped. To facilitate comparisons, libraries were also sequenced to 1000x average coverage using conventional paired-end sequencing.

Results: Sequence data were generated from 229 channels out of 276 that passed quality control. A total of 22,839 reads corresponding to 7.6 Mbases of sequence were generated in a six hour run and had a mean length of 338bp, consistent with FFPE library template size. Using discontiguous-megablast 1.3% of total reads mapped to the human genome. Of mapped reads an average of 88% of bases aligned to the reference, consistent with an overall error rate of approximately 12%. There were an average of 2 open gaps per read, suggesting that insertions and deletions were the most common error mode. The Burrows-Wheeler Aligner (BWA) failed to map reads.

Conclusions: We report the first demonstrated use of nanopore sequencing to analyze DNA obtained from target-enriched, clinically-derived, formalin-fixed tissue. While these results indicate that use of nanopore sequencing with current hybrid capture,gene-panel enrichment is limited, and not ideal for current clinical gene panel-based sequencing, such technologies may still serve as an inexpensive method for point-of-care molecular genetic testing using more focused enrichment methods and specialized analytic software.

2091 Mutational Analysis of the EGFR Tyrosine Kinase Domain Using a Shifted Termination Assay (STA) Fragment Analysis in Lung Cancer

Peter Miller, Naila Bhatri, Sugganth Daniel. The George Washington University Hospital, Washington, DC.

Background: Lung cancer is the leading cause of cancer deaths worldwide. Approximately 15% of patients, most often non-smokers with lung adenocarcinoma have tumor associated EGFR mutations.Shifted Termination Assay (STA) is a two-step PCR primer extension method that differentiates between wild-type (WT) and mutant sequences by amplification and selective extension with second step detection primers.

Design: 21 cases of lung adenocarcinoma were selected based on documented test results. DNA was extracted with the QIAamp FFPE kit from 4µ sections of FFPE tissue. The STA from TrimGen Corp, MD was used to detect point mutations in Exon18, 20, 21, deletions in Exon19 and insertions in Exon20 on the ABI 3500 platform. The STA was compared to PCR amplification and bidirectional gene sequencing of exons 18-21 for clinical validation of this assay. 6 genomic validated reference standards from Horizon Dx™ UK were also tested. Limit of detection was assessed with dilutions of the genomic standards with WT DNA at 50, 30, 10, 5 and 1%. Precision was measured on 20 inter and intra-run comparisons.

Results: 10 cases were detected to have EGFR mutations: 4 with L858R, 5 with 746 ΔLRE and 1 with S768I in exon 20. 11 cases tested negative. The STA results were in complete concordance with bi-directional sequencing. The 6 reference standards were WT, L858R, 746 Del, L861Q, G719S and T790M and these were correctly assessed on STA. The limit of detection runs estimated analytical sensitivity at 5% for deletions and 10% for point mutations. Precision was estimated at 100%.

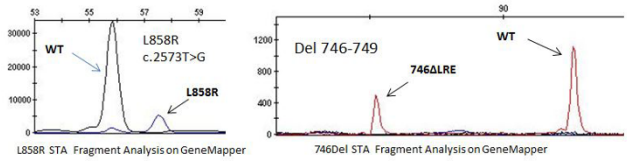

Conclusions: The STA for EGFR is a reliable assay for mutational testing in lung cancer. Its performance compares favorably with bi-directional sequencing and quantitative PCR methods. The STA covers approximately 99% of possible EGFR mutations and is highly suited for clinical use owing to its robust performance on the widely available ABI platform and ease of interpretation. The CAP IASLC guidelines recommend that mutations with a frequency of 1% or more be tested, in this regard the addition of detection primers for exon 19 insertions on the STA is currently in development.

2092 Quantum Dot Multiparametric Analysis of Colorectal Adenocarcinoma: Critical Examination of Expression Pattern Scoring Methods

Andres Moon, Rami Yacoub, Roberd Bostick, Peter Campbell, Alton Farris. Emory University, Atlanta, GA; American Cancer Society, Atlanta, GA.

Background: Molecular pathogenesis can be understood using numerous techniques; and immunohistochemistry (IHC) has an important role, particularly in anatomic pathology laboratories. IHC provides critical diagnostic, theranostic, and prognostic data; however, multiparameter IHC staining can be limited by technique restrictions and the amount of tissue available. Quantum dot IHC (QD-IHC) allows assessment of multiple parameters, allowing inclusion of more markers on the same slide than typical IHC.

Design: A QD-IHC panel containing 30 markers considered important in colorectal adenocarcinoma pathogenesis was developed with 5 markers/slide. Various approaches were employed in scoring 10 cases, including a modified H score (HS), a simple 0–3+ scale (SS), and image analysis (IA) using a customized implementation of the computer program Icy for nuclear isolation with intensity quatitation. Several statistical methods were employed in assessing the scoring systems, including linear regression (r), principal component analysis, and cluster analysis.

Results: All markers showed an expression range (Figure), and the same general trend was seen for all scoring methods. Computerized IA was developed to provide semi-automated reproducible results. Greatest agreement was seen between the IA and SS (mean r= 0.67, interquartile range [IQR]= 0.53-0.82), followed by SS and HS (mean r= 0.46, IQR= 0.21-0.71), and last by IA and HS (mean r= 0.41, IQR= 0.19-0.72). For nuclear staining, dynamic range was greatest using the HS, followed by SS, and IA (range/mean= 3.40, 2.56, 1.23, respectively). Principal component and cluster analysis showed that many markers in the same pathway were related.

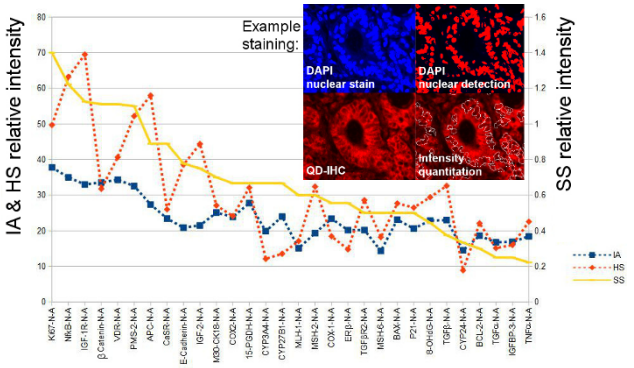

Conclusions: The QD-IHC method can be used to interrogate multiple markers simultaneously, providing an assessment of tissue expression while preserving architectural relationships. Various analysis techniques can be utilized, including an IA technique presented here that is conducive to automation. In this pilot study, QD-IHC shows promise, particularly when determination of tissue expression decides the therapeutic approach toward pathway inhibition.

2093 Chromogenic In Situ Hybridization of FGF23 mRNA in Phosphaturic Mesenchymal Tumors

Kent Newsom, John Reith, Dongtao Fu, Wonwoo Shon. University of Florida, Gainesville, FL.

Background: Oncogenic osteomalacia is a very rare paraneoplastic condition frequently associated with a distinct mesenchymal neoplasm, so-called phosphaturic mesenchymal tumor. Fibroblast growth factor 23 (FGF23) is established as the most common causative phosphatonin in tumor-induced osteomalacia. For FGF23 detection, several investigators have used immunohistochemistry and PCR-based technique; however, they may either be too nonspecific (immunohistochemistry) and overly sensitive (PCR). Recently, a highly sensitive and specific chromogenic *in situ* hybridization assay for *FGF23* mRNA has been studied. To assess its validity and reproducibility, we further evaluated *FGF23* mRNA expression in our institutional cases of phosphaturic mesenchymal tumor using this novel technique.

Design: Formalin-fixed, paraffin-embedded whole tissue sections from 7 phosphaturic mesenchymal tumors, with all but one case displaying clinically apparent oncogenic osteomalacia, and 12 histologic mimics/control cases (4 aneurysmal bone cysts, 4 chondromyxoid fibromas, and 4 osteoblastomas) were retrieved from our surgical pathology archives. Chromogenic *in situ* hybridization for *FGF23* mRNA was performed using the RNAscope® 2.0 FFPE Assay (ACD Inc. Hayward, CA). Intracellular staining was scored as "positive" using a previously validated scoring method by Carter et al (3+: ≥50% positive lesional cells; 2+:25-49% positive lesional cells; 1+: 10-24% positive lesional cells; rare 1-9% positive lesional cells).

Results: Morphologically, all tumors showed typical features of phosphaturic mesenchymal tumor (of the mixed connective tissue type) characterized by small and bland-appearing tumor cells embedded in a highly vascular and vaguely chondroid and "grungy" calcified matrix. All cases (7/7) were positive for *FGF23* mRNA (3+: 3 cases 2+: 2 cases; 1+: 1 case; and rare: 1 case). In control cases, *FGF23* mRNA was completely negative within the lesional tumor cells (0/12). Similar to previous observation, rare non-neoplastic osteoblasts/osteocytes revealed detectable *FGF23* mRNA in one case of aneurysmal bone cyst.

Conclusions: In our evaluation of *FGF23* mRNA chromogenic *in situ* hybridization assay, we found that the presence of *FGF23* mRNA expression was highly sensitive and specific for the diagnosis of phosphaturic mesenchymal tumor in patients with oncogenic osteomalacia. This novel assay permits direct visualization of transcripts within the context of tissue morphological observation and overcomes many limitations of other available techniques.

2094 Automatic Diagnosis of Prostate Cancer Using Quantitative Phase Imaging and Machine Learning Algorithms

Tan Nguyen, Shamira Sridharan, Virgilia Macias, Krishnarao Tangella, Andre Kajdacsy-Balla, Minh Do, Gabriel Popescu. University of Illinois at Urbana-Champaign, Urbana, IL; University of Illinois, Chicago, IL; Christie Clinic, Urbana, IL.

Background: Recent work has shown that refractive index measurements from the quantitative phase imaging (QPI) modalities can offer very competitive medical diagnosis results compared to those from Hematoxylin and Eosin (H&E) stained images. We demonstrate the first time to our knowledge, the use of QPI images obtained from the Spatial Light Interferometry Microscopy (SLIM) to do automatic prostatic cancer diagnosis.

Design: From a dataset of 240 prostate tissue cores, we built a machine learning algorithm to segment different regions of the biopsies (e.g. glands, stroma and lumen) based on the tissue's textural behavior in QPI images. Using the labeled maps, another automated step is applied to determine the diagnosis. To determine whether the tissue is benign or malignant, we utilize the textural information in the transition area between the gland and stroma and information around the gland's boundary. These features target

underlying morphological changes influenced by the existence of basal cell layers and textural difference generated by enlarged nuclei in cancerous cases. We also show how Gleason score can be obtained automatically with our method.
Results: Using the above method, we show an area under the receiver operating characteristic curve values of at least 0.96, 0.94, 0.87, 0.97 0.98 in discriminating between gland vs. stroma in cores with Gleason grade of 3+3, 4+4, 5+5, benign and High Grade Prostatic Intraepithelial Neoplasia respectively. From these labeled maps, using standard SVM classifier and the final patient diagnosis based on biopsies as the groundtruth, we report the average classification accuracy of 75% for Gleason grade 2 vs 3 and 70% for Gleason 2 vs 4. The accuracy of discrimination between grade 3 and 4 of up to 80% is reported for a smaller subset where diagnosis groundtruth per core is available.
Conclusions: In conclusion, our method is comparable to H&E images but it requires less time for sample preparation and has high throughput. The image contrast of QPI is intrinsically better for stromal region and invariant to the sample preparation or imaging conditions. This information is especially important to improve accuracy of automated diagnoses.

2095 Validation of PD-L1 Antibodies for Immunohistochemistry on Formalin Fixed, Paraffin Embedded Human Tissues

Edwin Parra, Barbara Mino, Erick Riquelme, Ximing Tang, Junya Fujimoto, Hui Liu, Jorge Blando, Jaime Rodriguez-Canales. University of Texas MD Anderson Cancer Center, Houston, TX.
Background: Programmed death-ligand 1 (PDL1) is a 43 KDa transmembrane protein which plays a key role in the modulation of the immune system. Recently it has been discovered that a wide variety of tumors can express PDL1. The recent development of new agents blocking the interaction PDL1/PD1 had opened a new therapeutic strategy for PDL1 positive tumors. In diagnostic pathology, it is essential to use well validated antibodies that can reliably detect the right PDL1 positive cases. Unfortunately, there are many PDL1 antibodies in the market which can provide questionable results, particularly for clinical use. Our goal is to compare and validate antibodies for PDL1 and identify those that can be reliably employed by the surgical pathologist.
Design: 5 commercially available PDL1 antibodies were tested, including clones EPR1161-2 (Epitomics), E1L3N (Cell Signaling Technology), 7G11, SP142 (Spring Bioscience) and a rabbit polyclonal (ab58810, Abcam). All antibodies were compared with clone 5H1 as a well validated reference antibody. For Western blot (WB) test, we employed protein extract from cell line 293 (negative) and 293-PDL1 transfected, including also several cancer cell lines. The antibodies that passed the WB test were then tested for IHC using FFPE cell pellets from the same cells 293 and 293-PD-L1 transfected, human placenta and tonsil. The staining pattern was also compared with the one from clone 5H1 as reference.
Results: Clones EPR1161-2, E1L3N and SP142 passed our WB test. Clones EPR1161-2 and E1L3N provided the same banding pattern observed with clone 5H1 characterized by a clean double band located in the 40-50 KDa region without extra bands. Clone SP142 instead showed a single band located in the 40 KDa region. Clone 7G11 showed multiple extra bands at different regions, while the polyclonal antibody showed multiple extra bands including the band at 40Kda. The IHC tests included clones EPR1161-2, E1L3N and SP142, and were compared with clone 5H1. All antibodies showed a similar membrane staining in the positive cells; however, antibody clones E1L3N and SP142 showed an identical staining pattern as clone 5H1 in all the tested samples. Clone EPR1161-2 instead showed cytoplasmic background and also staining in a large lymphoid cell population not observed in clones 5H1 and E1L3N.
Conclusions: From all antibodies tested the only commercially available antibodies that provide an identical staining pattern as clone 5H1 are clones E1L3N and SP142. Due to the exact identical WB banding pattern and IHC staining pattern, we selected clone E1L3N for pathology IHC.

2096 Development of 2D Cell Strain and 3D Tumor Spheroid Models for Precision Medicine

Chantal Pauli, Myriam Kossai, Jonathan Pauwels, Nikolai Steklov, Rema Rao, Andrea Sboner, Kenneth Hennrick, Brian Robinson, Juan Miguel Mosquera, Himisha Beltran, Mark Rubin. Institute for Precision Medicine of Weill Cornell Medical College and New York Presbyterian Hospital, New York, NY; Weill Cornell Medical College of Cornell University, New York, NY.
Background: Precision cancer medicine attempts to align tumor genetic changes with the most effective treatment. This tailored approach to cancer care will require model systems to help screen for ideal drugs and drug combinations. A high failure rate of drug candidates can be attributed in part to the use of 2D monolayer cultures that frequently produce inaccurate results and do not predict chemoresistance. The ability of 3D cultured tumor cells to recapitulate tumor-like microenvironment suggests that engineered tumor models may provide more accurate and reproducible information for drug testing. To address this, we have a program to develop patient-derived 2D cell strains and engineered 3D tumor spheroids for patient tumor specific drug testing.
Design: Fresh tissue samples from 18 different solid tumors were digested in Type II/IV Collagenase (Gibco), then re-suspended in Matrigel (BD), plated on plastic, and overlaid with cell type specific cell growth media, which consists of either serum free or FBS enriched DMEM/F12 (Gibco) with multiple growth factors optimized to propagate benign primary tumor cells. Cultures were maintained at 37°C in 5% CO2. Once established, specific drug testing was performed following 3 models: 2D monolayer culture, 2D monolayer culture converted into a 3D system (Biomatrix 3D®) and in Matrigel engineered 3D tumor spheroids.
Results: From 18 initial samples, our success rate in generating 2D cell strains and 3D tumor spheroids was about 30%-40%, with tumor content in biopsy as a major factor. We established 7 continous 2D and 3D cultures derived from distinct primary and metastatic cancers including prostate, kidney, bladder and endometrium, as well as sarcomas and a neuroendocrine tumor. Histology and cytology examination demonstrated that 3D tumor spheroids recapitulate harvested tumors. Next generation sequencing showed the presence of the same genomic alterations compared with original tumor without generating additional mutations.
Conclusions: We have developed individual patient-derived 2D cell strains and 3D engineered spheroids for tumor specific drug testing. The essential role of the pathologist in characterization of the 2D and 3D cultures is highlighted. This effort has been implemented for precision cancer care and clinical trials at our institution.

2097 KRAS Variants in Different Tumor Types: A Study Using Next-Generation Sequencing (NGS)

Kirsten Pierce, Juan Putra, Francine de Abreu, Jason Peterson, J Marc Pipas, Kerrington Smith, Gregory Tsongalis, Xiaoying Liu. Dartmouth-Hitchcock Medical Center, Lebanon, NH.
Background: The KRAS oncogene has been extensively investigated due to its role in numerous neoplastic pathologies. NGS is increasingly being used as a clinical tool to characterize tumors with precise information about their genetic composition. The value of mutational analysis in the prognostic and therapeutic evaluation of patients with tumors containing KRAS mutations is a controversial and continuously evolving concept. Current guidelines recommend testing for KRAS mutations in colorectal cancers to determine resistance to anti-EGFR therapies, however data is inconclusive regarding routine testing in cancers of other origins. Our aim was to study the prevalence of KRAS variants in tumors of various organs.
Design: 91 cases of lung adenocarcinoma, 67 cases of colorectal cancer and 2 glioblastomas were sequenced using the Ion Torrent Ampliseq Cancer Hotspot Panel v2 on the PGM sequencing system. DNA was extracted from unstained formalin-fixed-paraffin-embedded tissue sections, and barcoded libraries were prepared using 10ng of DNA. Samples were multiplexed on Ion Torrent 318v2 sequencing chips. Variant calling was performed using the Torrent Suite Variant Caller Plugin (v.4.0.2). Further annotation and functional predictions were assessed using Golden Helix SVS (v.7.7.8).
Results: KRAS mutations occurred primarily in codon 12 in both lung (84%) and colon (66%) tumors, as well as in 1 of the 2 glioblastomas (G12V). G12C was the most common variant in lung, compared to G12D in colon. Nearly a quarter of colon cancers were affected by a G13D mutation. Mutations in codon 146 (A146T and A146V) and codon 14 (V14I) were seen only in colorectal tumors. Mutations in codon 61 were seen glioblastoma (G61K) and lung (Q61H and Q61L), but not in any of the colon tumors.
Conclusions: Understanding the distribution of KRAS variants among different tumor types increases the recognition of the neoplastic pathologies that occur as a result of KRAS mutations. As NGS becomes an increasingly used tool in the clinical setting, incorporation of this knowledge can lead to more personalized patient care and improved health outcomes.

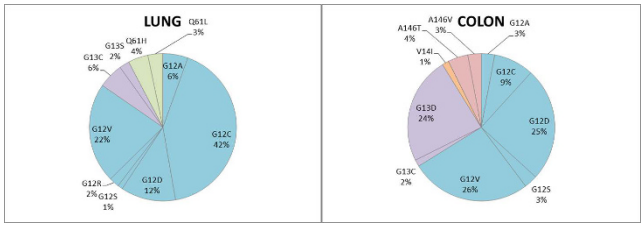

2098 A New Rabbit Monoclonal Antibody To Serine 10 Phosphorylated-Histone H3 (pHH3): An Immunohistochemical Comparison Study With a Rabbit Polyclonal pHH3

Weimin Qi, David Tacha, Ding Zhou, Heungnam Kim. Biocare Medical, Concord, CA.
Background: Phospho-histone H3 (pHH3) is phosphorylated during mitosis. The IHC staining of a Serine 10 (Ser 10) pHH3 has been reported to help predict prognosis in melanoma. Most pHH3 publications have used a commercially available rabbit polyclonal pHH3 (P) antibody; however, a monoclonal pHH3 offers an advantage of a specific epitope.
Design: A rabbit monoclonal (RM) antibody to Ser 10 pHH3 [BC37] was developed and confirmed by Western blot and ELISA. A blocking experiment was conducted on both antibodies using a phospho and non-phospho histone peptide to determine specificity for phosphorylation at Ser 10. Three cases of tonsil and melanoma were selected for IHC evaluation.
Quantification of pHH3 positive cells
pHH3 staining was recorded by counting five fields of view with a 20x objective. Quantitation of the pHH3 mitotic figures was calculated by using a computer assisted imaging system to count mitotic figures in prophase, metaphase, anaphase and telophase.
Results: In tonsil, the pHH3 (RM) displayed strong staining intensity without granular staining in interphase nuclei (figure 1) . However, the pHH3 (RM) showed only a slight reduction in staining percentage of mitotic figures when absorbed against the non-phosphorylated Histone H3 peptide, thus demonstrating its phospho-specific binding site (Table 1). Conversely, the pHH3 (P) antibody showed a significant reduction of staining in certain nuclei, thus was interpreted as not completely phospho-specific (Table 1). Mitotic counts in melanoma were similar with both pHH3 antibodies (Table 1).

Table 1

Tonsil	Cells Counted	Mitotic Figures	% Stained
pHH3 (RM)	15639	219	1.4
pHH3 (RM) Peptide	16431	197	1.2
pHH3 (P)	15510	381	3.1
pHH3 (P) Peptide	15909	270	1.7
Melanoma			
pHH3 (RM)	16479	148	0.9
pHH3 (P)	17517	180	1.0

Figure 1

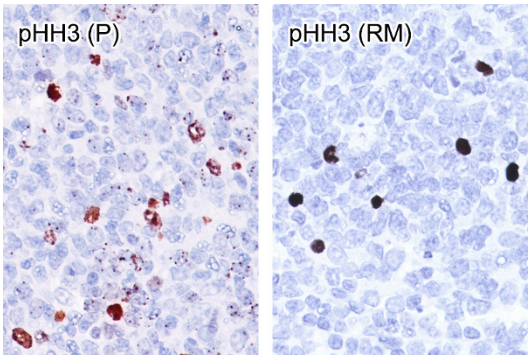

Conclusions: The rabbit monoclonal pHH3 demonstrated strong and specific staining for mitotic figures. Its mono-specificity to a targeted epitope is a clear advantage to its polyclonal counterpart that has a higher potential for cross reactivity due to recognizing multiple epitopes and potential staining inconsistencies caused from batch to batch variations.

2099 A Do-It-Yourself, High-Throughput Microdissection System for Improving NGS Data

Avi Rosenberg, Michael Armani [lrm], Patricia Fetsch, Liqiang Xi, Tina Thu Pham, Mark Raffeld, Yun Chen, Neil O'Flaherty, Rebecca Stussman, Adele Blackler, Qiang Du, Jeffrey Hanson, Mark Roth, Armando Filie, Michael Roh, Michael Emmert-Buck, Jason Hipp, Michael Tangrea. Johns Hopkins School of Medicine, Baltimore, MD; National Cancer Institute, Bethesda, MD; University of Michigan, Ann Arbor, MI; Sinai Hospital, Baltimore, MD.

Background: Manual macrodissection and laser-based microdissection technologies are user-driven methods that selectively recover histological regions or cells from cytology preparations and tissue sections. Yet, macrodissection is the dominant tool for laboratory-based studies and clinical applications, due to the high-cost and time-intensiveness of laser dissection. We present the first low-cost, do-it-yourself expression microdissection (DIY xMD) kit that combines the ease-of-use of manual methods with the precision of laser-based instruments.

Design: The DIY xMD kit is composed of an ethylene vinyl acetate (EVA) film, a vacuum bag system for optimal contact between the stained targets and the EVA film, and a broad-spectrum, handheld flashlamp. The total components of the system cost less than $500 USD.

Results: Using DIY xMD, we successfully isolated various targets, including immunostained epithelium, p53+ and ER+ nuclei, EBER+ and GFP+ cells, and GMS stained fungi from heterogenous samples. To demonstrate the molecular diagnostic advantage of rapid microdissection, we isolated a target cell population (at 5% cellularity), consisting of either melanoma or lung carcinoma cells, from an admixed cytospin sample. Next-generation sequencing (NGS) was performed on the xMD isolated target cells and compared to manual macrodissection of the whole sample. The xMD-isolated targets exhibited a 13-30-fold increase in mutation enrichment over the manually dissected samples. Specifically, the BRAF and KRAS mutations showed dramatic differences. The heterozygous BRAF mutation was not detected in the manual macrodissected admixed cytospin containing the melanoma cells, yet the xMD sample showed a mutation frequency of 52.3%. Likewise, the homozygous KRAS mutation frequency of the lung carcinoma admixed sample was 4.9%, but the xMD sample demonstrated a KRAS mutation frequency of 67.4%.

Conclusions: We demonstrate the significant potential of xMD enrichment for improving NGS detection for molecular diagnostics and precision medicine. This new system allows for high-throughput, efficient microdissection that is accessible to investigators and clinicians throughout the world.

2100 Limited Intratumoral Heterogeneity in Invasive Breast Cancer Genomic Drug Targets

Jeffrey Ross, Kai Wang, Roman Yelensky, Adrienne Johnson, Lily Khaira, James Sun, Bati Katzman, Tina Brennan, Caitlin McMahon, Kyle Gowen, Sohail Balasubramanian, Juliann Chmielecki, Siraj Ali, Julia Elvin, Doron Lipson, Vincent Miller, Philip Stephens. Albany Medical College, Albany, NY; Foundation Medicine Inc, Cambridge, MA.

Background: Tumoral heterogeneity (TH) has been a concern for clinicians and investigators, especially for diseases like invasive breast cancer (IBC) where needle biopsies may be tested to determine a patient's targeted therapeutic options. We applied a sensitive comprehensive genomic profiling assay to ten individual intratumoral biopsy sections from each of five IBC to determine the extent of TH amongst IBC genome derived drug targets.

Design: Ten biopsy sections from five IBC underwent comprehensive genomic profiling for hundreds of known cancer genes using the FoundationOne™ assay. Two separate non-adjacent FFPE blocks of the primary invasive duct carcinoma were sectioned from the block surface, one-fourth, one-half, three-fourths through the block and the deepest section possible and genomically profiled (fifty sections total). Samples were evaluated for all classes of genomic alteration.

Results: Profiling was performed on 4 IBC prior to therapy and 1 IBC post neoadjuvant treatment. The median patient age was 63.8 years. All IBC were high grade and > 2.0 CM (pT2). Two IBC were ER+/PR+/HER2-, 2 IBC were ER-/PR -/HER2- and 1 IBC was ER-/PR-/HER2+ (FISH). Only a single IBC case showed significant heterogeneity where variants were present at an allele frequency consistent with subclonal mutation. This case also harbored a hemizygous *TP53* deletion in 5/5 sections of block 1 but a homozygous *TP53* deletion in all five sections of block 2. Overall, heterogeneity was low across the nine druggable genes altered (*BRAF, BRCA2*, *CCND1*, *ERBB2*, *IDH2*, *NF1*, *PIK3CA*, *PTEN*, and *STK11*) with an overall concordance of 93%. The two drug targets that were discordant, *BRAF* and *PIK3CA,* had a concordance of 90% and 86%, respectively.

Conclusions: When a sensitive comprehensive genomic profiling assay is used, the intratumoral heterogeneity of druggable targets for IBC is limited. This data supports the use of comprehensive profiling of a single biospsy section to identify therapeutic targets to be appropriate in the majority of IBC patients.

2101 Stain-Free Detection and Quantification of Bone Marrow Fibrosis Using Two-Photon Excitation and Second Harmonic Generation Microscopy

Leslie Rowe, Ali Etman, Jessica Kohan, Josef Prchal, Gideon Ho, Dong Quan Liu, Mohamed Salama. ARUP Institute for Clinical and Experimental Pathology, Salt Lake City, UT; University of Utah, Salt Lake City, UT; Histoindex Pte Ltd, Beijing, China.

Background: Conventional evaluation of fibrosis in bone marrow from myeloproliferative neoplams (MPNs) is performed on reticulin and trichrome stained slides and is semi-quantitative and subjective due to inter-observer variability. Two-photon excitation microscopy (2PE) provides multi-dimensional optical sectioning in unstained tissue sections. When combined with second harmonic generation (SHG) simultaneous imaging of nonlinear structures, including fibrillar collagen, is possible. We investigated the applicability of two-photon microscopy (2PE/SHG) for quantifying fibrosis in unstained bone marrow core biopsy samples and compared its performance to the European consensus (EC) scoring system as well as a stereology-based quantitative method.

Design: Eight bone marrow core biopsy samples were identified for study inclusion. Unstained 4µm sections underwent 2PE/SHG imaging (Genesis® 200, Histoindex Pte. Ltd.) using a 20x objective to acquire multi-tiled images. Analysis was performed using proprietary imaging software. Parameters assessed included 2PE/SHG ratio, aggregated fiber percentage, total number, area, width, and length of fibers and number of fiber cross-links. The same slides were stained with reticulin, scanned using the Aperio ScanScope (Leica, Vista, CA), and analyzed using an approach adopted from stereology that quantifies fiber length density (FLD). EC scores were rendered on the reticulin stained slides by an experienced hematopathologist and ranged from 0 to 3+ fibrosis.

Results: 2PE/SHG imaging segregated bone marrow core cases with fibrosis from those without fibrosis. Binomial logistic regression showed significant correlation with EC for 2PE/SHG ratio (ρ=0.054); aggregated fiber percentage (ρ=0.015); fiber number (ρ=0.023); fiber area (ρ=0.004); fiber width (ρ=0.016) and fiber length (ρ=0.008). Interestingly, FLD using a stereology-based approach also showed significant correlation (ρ=0.001) with the EC. Cross-linking of fibers showed a trend but did not reach statistical significance (ρ=0.062).

Conclusions: 2PE/SHG imaging is a promising novel technology to be applied in quantification of marrow fibrosis, with performance equivalent to a stereology-based approach. Further studies with large sample size are needed to validate the utility of this method, however; several parameters can now be evaluated as well as compared to the biology of MPNs.

2102 Cost-Containment Protocol for Prostate Core Needle Biopsy: Grossing To Slide Processing

Roberto Ruiz-Cordero, Alia Gupta, Oleksandr Kryvenko, Richard Cote, Merce Jorda. University of Miami Hospital, Jackson Memorial Hospital, Miami, FL.

Background: Prostatic carcinoma (PCa) is the most common cancer in men in the US. It accounts for 1 in 4 newly diagnosed cancers each year. The estimate for 2014 in the US is about 233,000 new cases. The 10-12 prostate core needle biopsy (PCNB) sampling protocol is the current standard of care due to a higher detection and lower false negative rates, providing more accurate information for localized therapy. Reimbursement cuts by the Affordable Care Act have impacted anatomic pathology laboratories. We propose a simple, rapid procedure to decrease procedural costs and maintain high-standard patient care.

Design: A retrospective review of all the pathology reports of PCNBs performed at our institution from August 2013 to September 2014 was performed. Our current protocol includes one PCNB per paraffin block. Based on a published estimate of $4.71 per case from grossing to slide in a manual + automated laboratory, we calculated the actual procedural cost per case and the total cost for the study period after determining the number of blocks used in each case. We estimated the hypothetical procedural cost if the number of PCNBs per block was reduced to 3. Each block should contain 2 inked (different colors) and 1 non-inked PCNBs. Results are reported in absolute and relative

frequencies with mean and standard deviation or median and intervals, appropriately. The difference between real and hypothetical cost was assessed using a Student's t-test.
Results: A total of 363 PCNB reports belonging to 355 men (65, 43-90 years) were included. The total number of slides used during the study period was 4406 (12, 2-24 slides). Our total annual procedural cost of PCNBs was $20,752.26. The hypothetical total cost was $7,225.14. The actual average cost per case was $57.16 (± $12.02) in contrast to the hypothetical average cost per case of $19.90 (± 4.22) when using the proposed protocol. Significant differences between all scenarios were observed (p=0.000). The average cost difference per case was $ 37.26 (SD: ±7.98).
Conclusions: The actual procedural cost could decrease by 65% with implementation of the proposed protocol in our institution. However, each particular laboratory should consider additional costs, such as increased grossing time, cost of ink, decreased histotechnician time, staining time, and supplies used after grossing when adopting this proposed protocol.The potential impact on global health care cost could be around $3.5 million per year.

2103 Comprehensive Assessment of Targetable Somatic Alterations in Cytologic Cell Block Material Using a Clinical, Hybrid Capture-Based, Next-Generation Sequencing Assay

Justyna Sadowska, Ahmet Zehir, Ryma Benayed, Marc Ladanyi, Oscar Lin, Maria Arcila. Memorial Sloan Kettering Cancer Center, New York, NY.
Background: Multigene mutational profiling is an integral part of patient assessment with solid tumors. For many patients, cytology cell blocks (CCB) may be the only tissue available, limiting testing options. While amplicon-based NGS approaches have emerged as a preferred method for samples with low DNA content, hybrid capture methods may offer superior performance for comprehensive mutation profiling and concurrent assessment of copy number alterations, +/- structural variants. Here we describe our clinical experience with CCB using a 341 gene, hybridization-capture NGS assay.
Design: We used a hybrid capture based NGS assay (MSK-IMPACT) to detect somatic alterations in 341 cancer related genes. Consecutive cytologic samples received for routine mutation analysis are included in this review. Samples were sequenced on an Illumina HiSeq 2500 and analyzed with a custom analysis pipeline as tumor/normal pairs.
Results: A total of 62 cytology samples were received for testing, 54 (87%) FNAs and 8 (13%) pleural fluids, all prepared as CCB. Most samples were from lung and breast malignancies (74%). DNA was extracted from 15 sections (5mm) each. 84% cases were successfully tested, 9 (14%) failed due to low tumor content or low DNA yields. Concurrent H&E's were reviewed and cell counts performed. Failed sample counts averaged 239 cells (range 10-270) while all successfully tested had over 1,000 cells each. Direct comparison with a set of 50 needle core biopsies showed similar failure rate of 13%. A comparison of several quality metrics from the aligned sequencing data, including read trimming, insert size and duplication rates as a proxy of DNA quality, did not show significant differences between cytology and biopsy samples. In addition to successful assessment of recurrent somatic mutations in routine testing, the NGS method detected 2 rearrangements in ROS1 (lung) and 3 amplifications of HER2 (breast) which could not be detected by FISH assays due to insufficient/inadequate material.
Conclusions: The comprehensive molecular assessment of FFPE cytologic material using hybridization capture-based, NGS assays is feasible and generally successful if >15,000 cells are available. A distinct advantage over other methods is that it provides concurrent assessment of a broad range of targetable genetic alterations including mutations, copy number alterations and recurrent structural variants in cases where sufficient material would be unavailable for multiple FISH studies in addition to mutation profiling.

2104 Advances in Three-Dimensional (3D) High-Frequency (HF) Quantitative Ultrasound (QUS) for the Detection of Metastases in Lymph Nodes of Breast, Colorectal and Gastric Cancers

Emi Saegusa-Beecroft, Jonathan Mamou, Daniel Rohrbach, Thanh Minh Bui, Alain Coron, Tadashi Yamaguchi, Michael Oelze, Gregory Kobayashi, Clifford Wong, Conway Fung, Masaki Hata, S Lori Bridal, Eugene Yanagihara, Junji Machi, Ernest J Feleppa. University of Hawaii, Kuakini Medical Center, Honolulu, HI; Riverside Research, New York, NY; UPMC Univ Paris 06, Paris, France; Chiba University, Chiba, Japan; University of Illinois, Urbana, IL.
Background: Conventional histology methods do not evaluate the entire LN volume due to sampling limitations. Macro- and micrometastases may be missed. Unlike B-mode ultrasound, 3D-HF QUS is an innovative, fast, reliable, operator-independent method of scanning the entire LN volume and identifying regions suspicious for metastases on freshly-excised surgical specimens.
Design: 301 freshly-excised LNs from 171 patients were randomly enrolled from cancer specimens (118 breast, 147 colorectal, and 36 gastric). 26-MHz ultrasonic echo-signal data were acquired over the entire 3D volume of each LN. 13 QUS parameters associated with tissue microstructure were evaluated. All LNs were step-sectioned at 50-µm intervals over their entire volumes and stained with H&E. Linear-discriminant analysis was performed to differentiate metastatic from non-metastatic LNs, and areas under ROC curves (AUC) were computed to assess classification performance. 3D cancer-likelihood images were generated and compared with co-registered slides.
Results: Classification gave excellent AUC values for all 3 cancer-types (table1). 3D cancer-likelihood images effectively depicted metastatic regions (figure 1).

3DHF-QUS results						
Cancer	#LN	#(%) Metastatic	AUC	95% CI	Sensitivity (%)	Specificity (%)
Breast	118	17(14)	0.83±0.048	0.74-0.93	100	50
					88	65
Colorectal	147	21(14)	0.96±0.019	0.92-1.00	100	73
					95	80
Gastric	36	6(17)	0.96±0.030	0.88-1.00	100	72
					83	90
Total	301	44(15)	0.90±0.024	0.85-0.94	100	41
					96	63

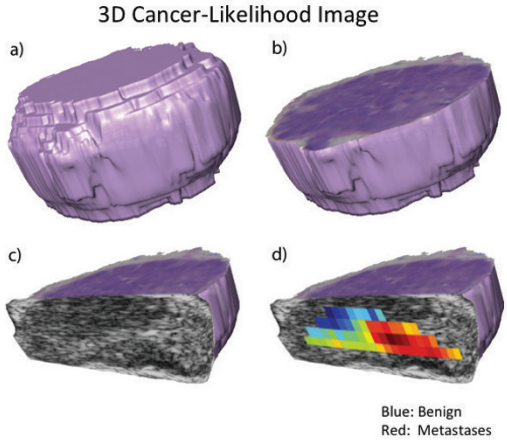

Conclusions: Operator-independent 3D HF-QUS allows reliable entire-volume LN evaluation for identifying metastatic regions on freshly-excised surgical specimens. The method can be implemented in a compact clinical instrument for pathologists to identify suspicious regions of nodes that warrant targeted histological evaluation.

2105 Evaluation of a New Rabbit Monoclonal Cocktail (EP17/EP30) for the Immunohistochemical Evaluation of CK8/18

Amaia Sagasta, Alfons Nadal, Jordi Farre, Pedro Fernandez. Hospital Clínic, Barcelona, Spain; University of Barcelona, Barcelona, Spain; Dako, Barcelona, Spain.
Background: There are several commercially available antibodies for low molecular weight cytokeratins (CKs) but they show slightly different reactivity patterns which may have diagnostic implications. We have evaluated the new anti-CK8/18 cocktail, clone EP17/30 (Dako), in comparison to other available antibodies against CK8 and CK18 in a large series of normal and neoplastic epithelia with special emphasis on tissues where CK8/18 is useful as an aid in the diagnosis.
Design: Cam 5.2 (Becton Dickinson), anti-CK8/18 (B22.1&B23.1, Cell-Marque) and anti CK8/18 (clone EP17/30, Dako) antibodies were optimized and tested under identical conditions on an automated platform. Antibodies were tested on 157 samples including normal epithelia and carcinomas from the digestive, respiratory and urologic tracts and breast carcinomas, arranged into tissue microarrays. Slides were digitalized for improved simultaneous evaluation. Additionally, a series of 26 cases previously analysed for Cam 5.2 as a diagnostic aid were tested with the above antibodies. Parameters evaluated were predominant intensity (0-4), highest intensity (0-4) and percentage of positive cells.
Results: All antibodies provided a good staining of most simple epithelia and derived neoplasms with predominant intensities usually 3 and 4. Cam 5.2 showed a more frequent 4 "predominant intensity" (Wilcoxon test, $p<0.02$) and EP17/30 a significantly higher mean percentage of positive cells in adenocarcinomas (paired T-test,$p<0.03$). EP17/30 also showed a significant more intense and diffuse positivity in renal clear cell and spindle cell carcinoma, squamous cell carcinomas of several locations and embryonal carcinomas.

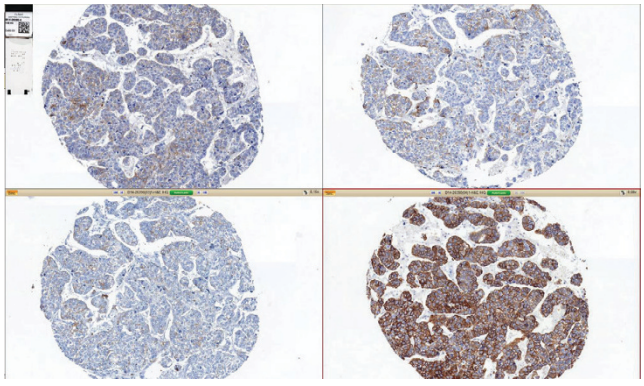

Clone EP17/30 outperformed the other antibodies in cases of mucinous tubular and spindle cell renal carcinomas, olphactory neuroblastoma, carcinosarcoma and a pleomorphic carcinoma by showing a higher percentage of positive cells (>20% increase) or being the only positive antibody.
Conclusions: Clone EP17/30, anti-CK 8/18 cocktail is a reliable alternative to other anti-low molecular weight CKs and can provide advantages in the diagnosis of some neoplasms due to its enhanced diffuse and homogenous staining.

2106 Promise and Perils of NGS Testing in Lung Cancer

Gulpreet Singh, Kimberly Walker, Linden Watson, Riyam Zreik, Robert Beissner, Arundhati Rao. Baylor Scott & White Memorial Hospital - Texas A&M Medicine, Temple, TX.
Background: Lung adenocarcinoma remains the leading cause of cancer death worldwide and accurate mutational status is important in selecting patients for targeted therapy. The rapidly expanding list of actionable targets makes next generation sequencing (NGS) an attractive cost effective option. We present a comparative study of the Pyromark Q24 assay and the Ion Torrent Hotspot panel.
Design: With IRB aprroval, 31 cases of lung adenocarcinoma (24 formalin-fixed, paraffin-embedded (FFPE) and 7 FNA smears) including 6 metastatic cases were retrieved, diagnosis confirmed, and patient chart reviewed. NGS was performed with the Ion AmpliSeqTM Cancer Hotspot Panel. Pyrosequencing was performed to confirm the NGS findings using the Pyromark Q24 pyrosequencer and the Qiagen EGFR and KRAS Pyro Kits.
Results: DNA extracted from FFPE samples ranged from 14.5-100 ng/ul and 6-18 ng/ul from FNA smears. All FNA smears yielded valid results. Overall, NGS and pyrosequencing showed concordant results in 26/31 (84%) cases and FNA smears were 72% concordant. NGS was discordant in 3/7 (43%) exon 19 deletions and 2/7 (28%) L858R mutations. 5 novel EGFR mutations were identified. 5 cases harbored KRAS mutations and were mutually exclusive of EGFR. The mean tumor size was 2.6 cm (range 0.7-6.5 cm) with a mean follow-up of 34 months (range 6-79 months). 5/6 (83%) patients with metastatic disease harbored mutations in EGFR and NGS detected 3/5 (60%) and one patient mets was KRAS positive on both platforms. 4 patients are deceased, 2 with L858R (1 TP53 and 1 ATM mutations), 1 with exon 19 deletion, and 1 with novel EGFR mutations and additional deletions and mutations in EGFR and TP53.
Conclusions: FFPE and cytology smears provide adequate tissue for molecular analysis. NGS had valid results obtained when the DNA content is above 15 ng/ul. The different mutations noted with the Ion Torrent might be a result of the documented insensitivity to deletions or bias in interpretation of homopolymers and may need either reconfirmation by a different assay or use of different algorithms to account for this bias. Progression while on therapy seemed to be associated with multiple EGFR mutations, TP53 and ATM mutations but is limited by the sample size.

2107 Development of a New Quantitative Proteomic Analysis of Amyloid Deposits: Preliminary Results

Jesus Sola, Fernando Corrales, Carmen Beorlegui, Angel Panizo, Jose Solorzano, Maria Mora, Ramon Lecumberri, Javier Pardo. Hospital San Pedro, Logroño, Spain; Clínica Universidad de Navarra, Pamplona, Spain; Complejo Hospitalario de Navarra, Pamplona, Spain; CIMA, Pamplona, Spain.
Background: In routine clinical practice, diagnosis and classification of amyloidosis is made in two steps. First, the presence of amyloid deposits in tissue biopsy has to be established and Congo red (CR) staining remains the gold standard method. Next, the protein composition (subtype) of the amyloid deposits is established by directly phenotyping the tissue with immunohistochemistry (IHC). Recently, non-supervised shotgun proteomic-based approaches have been proposed to identify the composition of amyloid protein upon tissue laser microdissection, with great impact in the choice of the clinical management options. The aim of this study is the development of a targeted, quantitative proteomic-based method Selective Reaction Monitoring (SRM) to identify the four most common forms of amyloidosis from formalin fixed paraffin embedded tissue samples (FFPET).
Design: Thirteen samples from different organs (heart 5, duodenum 2, lung 1, lymph node 2, liver 1, breast 1, adipose tissue 1) were analyzed. Eleven of them were amyloidosis and two light-chain deposit disease. All samples were tested by SRM, and 5 among them were also analyzed by shotgun proteomics upon laser microdisecction. For SRM, 1 to 6 unstained 10-micron sections were scrapped, resuspended in buffer and proteins were extracted by sonication. Upon tryptic digest and peptide pre-purification, reverse phase chromatographic separation was performed on a nanoHPLC connected online to a 5500 QTRAP triple quadrupole mass spectrometry to monitor the protein-specific transitions.
Results: Accurate results were obtained in all cases, with perfect correlation between microdisection-shotgun and whole tissue-SRM methods From the amyloid cases 5 were light-chain (2 lambda, 3 kappa), 2 SAA and 4 transthyretin (1 mutated transthyretin). The two cases of light-chain disease were positive for kappa or lambda but negative for other components of amyloid, like APOE1 and P-protein.
Conclusions: The targeted proteomics approach reported here increases the accuracy of detection and allows quantitation of pathogenic proteins from amyloid deposits extracted from FFPET. Moreover, no laser microdissection is required, which simplifies the overall procedure and facilitates its incorporation to the clinical routine. The method is currently being developed to allow absolute quantitation of the targeted proteins.

2108 Quantitative Phase Imaging: A Novel Colon Cancer Screening Tool

Shamira Sridharan, Jon Liang, Virgilia Macias, Anish Shah, Roshan Patel, Krishnarao Tangella, Grace Guzman, Andre Kajdacsy-Balla, Gabriel Popescu. University of Illinois at Urbana-Champaign, Urbana, IL; University of Illinois, Chicago, IL; Christie Clinic, Urbana, IL.
Background: Spatial Light Interference Microscopy (SLIM) is a quantitative phase imaging (QPI) method that measures the refractive index distribution in unstained tissue using white light. Scattering parameters measured using QPI have been used to diagnose prostate cancer, perform Gleason grading and predict recurrence of prostate cancer after prostatectomy. We now show the potential of QPI as a quantitative colon cancer screening tool.
Design: We imaged 383 unstained tissue microarray cores, which included tissue from 4 classes: normal, hyperplasia, dysplasia and colon cancer, using the 40X/0.75NA objective of the SLIM system. The phase distribution in 455 normal and 194 cancerous glands from 120 cores was used to train the support-vector machine algorithm on MATLAB. The results from the training set were used to classify 2252 glands from 262 cores in the testing set into high suspicion (dysplasia or cancer) and low suspicion group (normal or hyperplasia).

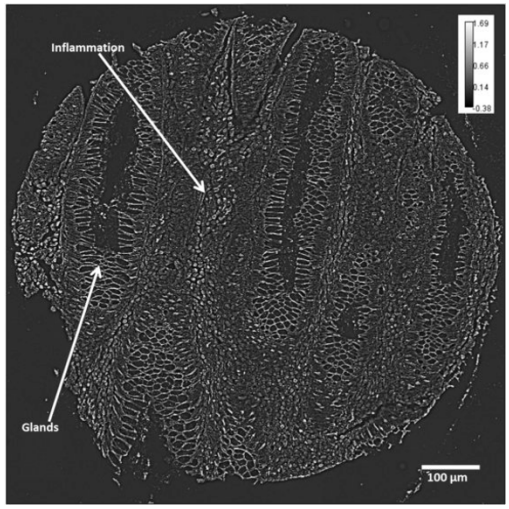

Results: 86.94% of 222 dysplastic glands and 82.49% of 794 cancerous glands were classified into the high suspicion group, whereas 91.52% of 248 hyperplastic glands and 80.57% of 988 normal glands were classified into the low suspicion group. When multiple glands in each core were grouped together, the classification accuracy improved to 93.33% in 30 dysplastic cores, 87.25% in 102 cancerous cores, 96.3% in 27 hyperplastic cores and 87.38% in 103 normal cores. The median of the phase distribution in glands can differentiate between cancerous and dysplastic glands with 68% accuracy.

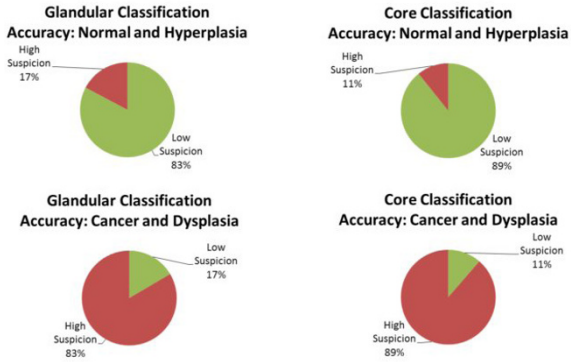

Conclusions: The accuracy of our classification method improves as the number of glands increases, so we expect the accuracy to be greater than 90% in biopsies. We are working to improve the distinction between dysplastic and cancerous colon glands. We believe QPI shows promise as a new colon cancer screening tool.

2109 Bone and Soft Tissue Extirpation: Whole-Specimen Freezing Delivers Superior Pathologic Evaluation

Veronica Taylor, Dora Lam-Himlin, Shipra Garg, Steve Taylor. Mayo Clinic Hospital, Phoenix, AZ; Phoenix Children's Hospital, Phoenix, AZ.
Background: In bone and soft tissue resections, serial slab sections are ideal for identifying margin status, size of tumor, and presence of discontinuous lesions. However, the variable density of bone and soft tissues creates a challenge for prosectors to reliably yield multiple intact thin slabs.
Design: Using a method of whole-specimen freezing and slab-sectioning, we prospectively processed 41 cases of bone and soft tissue resections between 2011 and 2014. Following removal of vascular/neurovascular margins, whole gross specimens were placed in a freezer (-70 to -140) for a minimum of 4 hours. Using a band saw, the frozen specimens were serially sliced at 4-8 mm intervals in the plane demonstrating maximum tumor burden as documented by radiological analysis. These intact slabs were

photographed and fixed in 10% formalin for 24 hours. Following soft tissue sampling, the slabs were decalcified, and subsequent bone sections were sampled and mapped to corresponding photographs. Histologic sections were retrospectively evaluated for freeze artifact, bone dust, thermal injury, and immunoreactivity.
Results: Slab-sectioning following whole-specimen freezing resulted in crisply visible anatomic relationships across multiple planes.

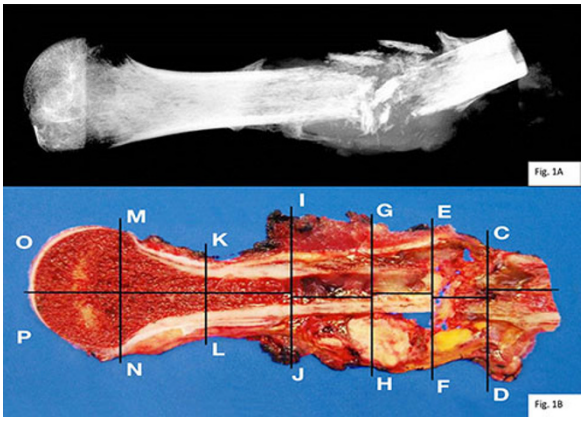

Pathologic fractures and both small and large joints remained intact with this method. Histologically, freeze artifact was present in 6 of 39 (15%) cases available for review, but was insignificant to interpretation and was not affected by freeze duration (up to 72 hours). No loss of immunoreactivity was seen (0 of 5 cases). Bone dust and thermal injury were not significant findings in any of the cases.
Conclusions: Whole-specimen freezing followed by slab-sectioning keeps the specimen vividly intact. These multiple thin sections allow for superior gross inspection, correlation with radiologic study, photographic documentation, and aids in the selection of histologic sections. The protocol is easy to follow, yields reproducible results and induces no significant freeze artifact, providing excellent histomorphology regardless of tumor type involving bone. We recommend slab-sectioning following whole-specimen freezing for all bone tumor resections and we offer our protocol in detail.

2110 Optimized Methodology for Molecular Testing of Cytological Biopsy Specimens

Shaozhou Tian, Maria Arcila, Roger Smith, Oscar Lin. Memorial Sloan Kettering Cancer Center, New York, NY.

Background: Molecular testing from fine needle aspiration biopsy (FNAB) specimens is increasingly requested and often the only available diagnostic specimen. However, downstream testing suffers significantly from preanalytical sample manipulation. We set out to optimize nucleic acid isolation from FNABs and establish the minimum number of cells required for high demand tests. The cornerstone of our approach is minimal sample manipulation by directly utilizing liquid preparations.
Design: Six cell lines were serially diluted to establish samples of 100,000 (100k), 10,000 (10k) and 1,000 (1k) cells in 1 mL of CytoLyt. A cytospin slide was prepared from a 100 uL aliquot from each sample. DNA was isolated from each preparation with the Qiagen DNeasy Tissue Kit. The number of cells observed in the cytospin slide in ten 10x powered fields was subsequently correlated with the DNA yield by Qubit.
Results: DNA isolated from the six cell lines ranged from 34.1 ng to 619.2 ng (mean = 328.9 ng) at the 100k cell preparations, up to 57.1 ng (mean = 35.5 ng) for the 10k cell preparations, and no measurable DNA for the 1k cell preparations. Aliquot cytospin counts ranged from 340-1148, 30-160, and 0-20 respectively in ten 10x powered fields. Linear regression analysis demonstrated that a cytospin aliquot count of 600 cells was needed for optimum (250 ng) DNA yields while as few as 30 cells yielded marginally sufficient (50 ng) material for high demand assays.

Cell Line	100k Cell DNA Yield (ng)	10k Cell DNA Yield (ng)	1k Cell DNA Yield (ng)	100k Cell Cytospin Count (Ten 10x pf)	10k Cell Cytospin Count (Ten 10x pf)	1k Cell Cytospin Count (Ten 10x pf)
BER	79.7	0	0	340	30	2
BOD	376.3	39.7	0	540	56	6
BZ	312	39.6	0	572	72	0
EO	552	26.6	0	568	84	0
HCC827	619.2	57.1	0	520	134	2
LP9	34.1	49.9	0	1148	160	20
Mean	*328.9*	*35.5*	*0*	*615*	*89*	*5*

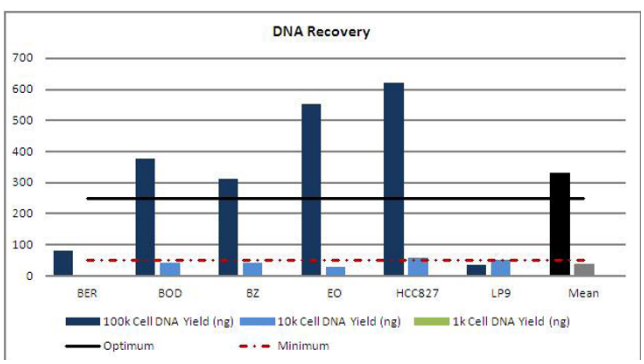

Conclusions: Direct DNA isolation from CytoLyt liquid preparations and morphologic assessment of the corresponding cytospin, represents not only a viable, but potentially superior method for optimized DNA isolation. We demonstrated that the 10k cell sample was at the threshold of most high molecular demand assays. The ancillary cytospin slides provided crucial information on tumor content and anticipated DNA recovery. The data suggests our protocol as a valuable approach to molecular testing in FNAB samples.

2111 Comparative Study of Different Modalities for the Evaluation of Ki67 Expression/Index in Estrogen Receptor (ER) Positive Invasive Mammary Carcinoma

Katrina Van Pelt, Erin Bascom, Brett Baskovich, Donna Dyess, Andrea Kahn. University of South Alabama Medical Center, Mobile, AL; University of South Alabama, Mobile, AL.

Background: Investigation of prognostic markers is needed to guide more effective therapy in breast cancer. The proliferation marker, Ki67, may stratify cases by aggressiveness and molecular subtype (luminal A vs. luminal B). There are multiple methods of estimating Ki67 index, however, they are highly variable and a standard has yet to be established. The objective of this study is to determine an effective method in a manner similar to neuroendocrine tumors.
Design: Following IRB approval, ER positive invasive breast carcinoma core or excisional biopsy specimens in adult female patients were identified from our 2010-2013 database. All previously-performed Ki67 immunohistochemically-stained slides were scanned by the DAKO ACIS image analyzer. An area of high proliferation (hot spot) was selected for analysis and quantified by three modalities: assisted manual (AM), image analysis (IA) and visual estimate (VE). First, the tumor nests were selected in the software and IA counts recorded. The selected area was then counted by AM method using the ImageJ cell counter plugin. A VE was obtained at 1% increments. The results were analyzed by comparing the three methods by linear regression and correlation statistical analysis. Cases were stratified into low (<14%) and high (≥14%) proliferation index (PI) using a previously-reported cutoff for each method.
Results: Forty-three cases were included in this phase of the study. VE was the most efficient method with the AM method being the most time-consuming. Based on AM counts the number of cells analyzed ranged from 421-2,808. The PI by AM counts, used as the gold standard, ranged from 1.99-66.52%, for IA ranged from 1.5-82.8%, and VE ranged from 1-80%. The correlation coefficient of IA versus AM was 0.86 and for VE versus AM was 0.82. When using the selected cutoff the PI was overestimated in 6 cases (14%) with IA and underestimated 9 cases (21%) using VE.
Conclusions: Our study shows that using a selected hot spot containing no less than 400 cells analyzed by an automated method, the proliferation index can be calculated in invasive breast cancer in an objective manner. There was a closer correlation between IA and AM methods compared to VE and AM methods. Additional studies and improved algorithms could allow for a more objective and reproducible estimation of the PI value.

2112 Utility of miRNA Detection By Rapid Chromogenic In-Situ Hybridization (CISH) on FFPE Samples in Surgical Pathology: Aiding in Diagnosis, Prognosis and Selection for Therapeutic Targets

Puneeta Vasa, Ashis Mondal, Abhishek Mangaonkar, Ravindra B Kolhe. Georgia Regents Univeristy, Augusta, GA.

Background: In last decade, a class of noncoding RNAs called miRNA's was identified as critical gene regulators in cell growth, disease, and development. miRNA's are cell specific, tissue specific and their expression very well correlates with the stage of the cancer or disease. As these non-coding RNA's they are in a very stable molecules & universally expressed in saliva, sputum, urine, bile and serum and hence great biomarkers. Similar to fluorescent in situ hybridization (FISH), in CISH a labeled complementary DNA or RNA strand/probe is used to localize a specific DNA/RNA sequence in a tissue specimen. It is used to evaluate gene amplification, gene deletion, chromosome translocation, and chromosome number.
Design: The miRNA expression profile of hepatocellular carcinoma (HCC), Plasmablastic lymphoma, diffuse large B-cell lymphoma and melanoma were evaluated using Affeymertrix miRNA microarray platform on GeneChip miRNA 3.0 array. Based on this data, miRNA probes for mir-21, mir-155, mir-196a and mir-221 were constructed or purchased from Biogenex & Exiqon. Manufactures protocol were followed. Nuclear & cytoplasmic mir-CISH stains were graded as: negative (-), weak (1+), moderate (2+) or strong (3+) and distribution was focal (<10%), patchy (10-50%) or diffuse.
Results: Neoplastic cells in HCC showed prominent nuclear staining for miR-21 in comparison to normal liver cells.

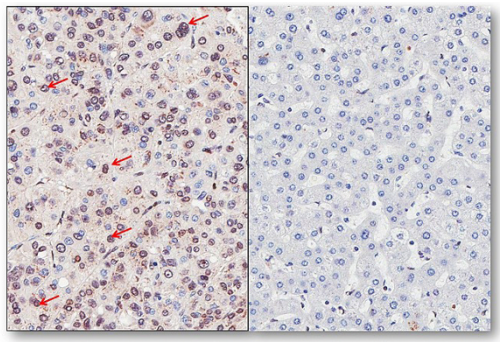

Strong mir-21 nuclear staining in liver cancer cells

Negative mir-21 staining in normal liver cells

Similar results were observed in other maligancies.

Conclusions: CISH is a cutting edge, cost-effective, & very valid alternative to FISH in testing for DNA/RNA alteration, especially in centers primarily working with IHC. CISH is a promising alternative to FISH because it has the advantages of being a method evaluated by bright-field microscopy and the generated chromogenic signals are also stable. Most importantly you can evaluate the cell morphology and locate the signals in CISH as compared to FISH. Methods of sub-cellular and tissue localization of mi-RNA's s are essential to understand their biological roles and their contribution to disease along with diagnosis.

2113 Loss of Antigenicity Due To Long-Term Storage Cannot Be Prevented By High Vacuum, Low Vacuum and Aluminum-Plastic

Ulrich Vogel. University Hospital, Eberhard-Karls-University, Tuebingen, Baden-Wuerttemberg, Germany.

Background: Especially paraffin tissue microarrays (PTMAs) are a powerful tool in translational research in pathology by allowing high throughput examinations and sparing labour and consumables. The often precious PTMAs should not be cut very often in order to prevent unnecessary tissue loss. Therefore, many sections are prepared at one sectioning procedure and stored for further use. However, as described in literature, those stored sections may experience loss of antigenicity in the course of time depending on the antigen studied and become useless or even misleading because of false negative results in immunohistochemistry. Several methods are proposed in literature to protect the antigenicity of the sections like paraffin coating, nitrogen storage and storage at a low temperature.

Design: A PTMA was constructed containing 29 breast needle biopsy specimens and 11 control and marker specimens. 2-3 µm thick sections were cut and immunohistochemically stained for the estrogen receptor, bcl2 (with biotin block) and ki-67 directly after sectioning, 9 and 12 months after being stored at room temperature in a wooden slide box, under high vacuum, low vacuum and a sealed plastic-aluminum bag. The immunohistological staining was performed on a BenchMark automatic stainer. The PTMA slides were scanned with a Mirax automated slide scanner. The cores of the slides were segregated with the Mirax Viewer and exported into jpeg-files. The cores of the differently stored slides were compared by eye at the computer screen for the number of stained cells and the intensity of the immunohistological staining.

Results: The intensity of the immunohistochemical staining diminished in the course of time due to loss of antigenicity. However, a striking loss of antigenicity could not be found for each antibody within 12 months. Slides stored in high vacuum seemed to have a slightly reduced loss of antigenicity in comparison to low vacuum, plastic-aluminum bag and wooden slide box. A good marker for tissue degradation due to long term storage was the reduced background staining in liver marker tissue and also in some tumor cell cytoplasms. Especially this reduced background staining may sometimes mislead the researcher at the first moment and simulates some loss of antigenicity because of a clear cytoplasm. Some changes in the thickness of the sections may also complicate the comparison of stained sections.

Conclusions: Antigen deterioration during long term storage cannot be prevented even with high vacuum, low vacuum and plastic-aluminum.

2114 Low Cost, Simple, But Nonetheless Precise Technique To Microdissect Cores From Tissue Microarray Slides for PCR Using Tesafilm® and a Biopsy Punch With a Plunger System

Ulrich Vogel. University Hospital, Eberhard-Karls-University, Tuebingen, Baden-Wuerttemberg, Germany.

Background: Tissue microarrays (TMAs) are a powerful tool especially in translational research in pathology. Besides immunohistochemistry sections of the TMAs can also be used for polymerase chain reaction (PCR) or reverse transcriptase PCR (RT-PCR) examinations. To extract the tissue from the TMA sections, the cores can be scraped off the slide with a sharp blade (e.g. surgical disposable scalpels or short self-made blades from microtome blades) and transferred to Eppendorf tubes for further processing. In case of paraffinized tissue sections the slides will be deparaffinized before the scrape procedure. A disadvantage of this technique is the sometimes difficult transport of the small, very light scraped tissue into the Eppendorf tube for further processing due to electrostatic effects by which the tissue will jump off the blade. Furthermore, scraping of tissue may be prone to contamination.

Design: 5 µm thick sections of a paraffin TMA filled with synovial sarcomas (diameter of the cores: 1.0 mm) were mounted on glass slides and deparaffinized using xylene. After a 100% ethanol step the slides were dried at room temperature. Then a commercially available, conventional tesafilm® was mounted on the top of the sections. A regular disposable microtome blade was cut to 2 cm in length using a band saw equipped with a diamond blade. With the shortened blade fixed in a pliers the tesafilm® and the cores were detached from the glass slide and transferred to a black paper sheet with the cores opposite to the paper surface. The cores were punched out together with the tesafilm® backbone using a disposible biopsy punch 1mm in diameter with a plunger sytem and transferred to Eppendorf tubes. After digestion with proteinase K RT-PCR was performed to detect the SYT-SSX fusion transcripts.

Results: The procedure of scraping the cores-tesafilm®-sandwich from the slide is easy to perform. Furthermore punching out the cores of the tesafilm® backbone and the transfer of the punched cores to the Eppendorf tube is not difficult. Even one core 1 mm in diameter is enough to get a strong band of the PCR product in the agar gel.

Conclusions: The use of tesafilm® as a backbone for deparaffinized TMA sections is an appropriate technique to retrieve cores for PCR/RT-PCR examinations with the advantage of a simple core handling and a reduced risk for contamination.

2115 Frozen Section (FS) Evaluation Via Telepathology (TP) in a Cancer Center Setting

Aram Vosoughi, Merce Jorda, Carmen Gomez-Fernandez, Monica Garcia, Andrew Rosenberg, Carol Petito, Jennifer Chapman, Offiong Francis Ikpatt, German Campuzano-Zuluaga, Cesar Llanos, Oleksander Kryvenko. University of Miami, Miller School of Medicine, Miami, FL.

Background: Prior FS TP experience has been limited to practices with spatially remote locations. At our center surgical pathologists rotate daily coverage of FS at two nearby locations. We reviewed all cases with FS over a one year period and evaluated the impact of TP on diagnostic accuracy and overall cost.

Design: Evaluated FS service was provided in a building 0.2 miles away across a busy 6-lane highway. Digital transmission was through a dynamic TP setting with a streaming resolution of 1360x1024 ppi and 15fps frame rate. Data were transmitted over a secure 1 Gbit/s local area network. A frozen section slide was driven by a resident directed by a faculty via phone. We analyzed all FSs and corresponding final reports and re-reviewed the discrepant cases. Descriptive statistics and chi-square test were used. In cases with multiple parts, each part was considered a separate event. For the number of travels in cases with multiple parts, we considered each batched reporting of parts as a separate event.

Results: From 642 specimens with FS, 333 (690 parts) were interpreted via TP and 319 (728 parts) via direct microscopy. There were 18 (2.6%) discrepancies, 7 (1%) sampling and 11 (1.6%) diagnostic errors, in TP cases and 24 (3.3%), 13 (1.8%) sampling and 11 (1.5%) diagnostic errors, in directly examined cases. The difference between the incidence of diagnostic errors (p=1.0) and sampling errors (p=0.26) was not significant between TP and direct microscopy. Among cases with diagnostic errors, 3 TP and directly examined misdiagnoses were due to overcall of benign lesions as malignant. Two TP and 1 direct examination undercalled cases with fungus. Six TP and 7 direct examination under called malignant lesions. Average round trip to the frozen section lab takes a pathologist approximately 20 minutes. For 333 cases performed with TP, 386 travels (128.7 hours) were required. Using the AAMC associate professor 50th % salary ($147.9 / h), time saving brought by TP was worth $ 18,930.00 over study period. The upfront capital cost for establishing a TP connection (hardware and software) was $ 8,924.00 and maintenance was limited to a regular microscope maintenance.

Conclusions: There is no difference in diagnostic or sampling error incidence between FSs reviewed by TP and direct microscopy in a setting of high incidence of FS. This diagnostic error is within the recommendation limit (<2%). Capital investments are rapidly amortized in a center with busy FS service.

2116 Investigating the Progression of Liver Disease To Hepatocellular Carcinoma Using Label-Free Chemical Imaging

Michael Walsh, Hari Sreedhar, Bennett Davidson, Lily Mei, Kyle Meinke, Grace Guzman. University of Illinois, Chicago, IL.

Background: Hepatocellular carcinoma (HCC) is the most common primary liver carcinoma. The disease typically develops in the context of liver cirrhosis from various etiologies, and shows a progression through intermediate stages of dysplasia to cancer. Current diagnosis of HCC is made by a pathologist on a stained tissue section from a liver biopsy, a process that is subjective and may not yield consistant diagnoses between pathologists. Infrared spectroscopic imaging through Fourier Transform infrared (FT-IR) and quantum cascade laser (QCL) imaging could offer a label-free chemical imaging approach to derive biochemical information from tissue biopsies. These data can be harnessed to allow for cell type and disease classification. In this study, we used high resolution IR imaging to diagnose the disease state in liver tissue the progression from cirrhosis to hepatocellular carcinoma.

Design: Samples were taken from tissue microarrays of liver biopsies from patients with non-dysplastic cirrhosis, low grade dysplasia characterized by large cell change, high grade dysplasia characterized by small cell change, and hepatocellular carcinoma. Unstained sections were scanned in IR, and serial sections were acquired for H&E staining. Diagnosis of disease state was made by a liver pathologist on the H&E images, and used to identify regions of hepatocytes in the above four disease states on the corresponding IR images and extract spectral data. A Random Forest spectral classifier was constructed to differentiate between these disease states on the basis of this data using 30 cores for training and 8 cores for validation.

Results: A Random Forest classifier of the four disease states was constructed to use the spectral data from the hepatocytes. It was able to accurately sort samples into non-dysplastic cirrhosis, large cell change, small cell change, and hepatocellular carcinoma. Furthermore, this was achieved without the use of any stains on the tissue section in an automated manner.

Conclusions: In this study, we demonstrated the ability of high definition IR imaging to classify liver disease stages in the progression to hepatocellular carcinoma. FT-IR and QCL IR imaging show the potential to be a powerful adjunct to current pathological procedures to aid in cases of difficult diagnosis and derive novel biochemical information about disease progression.

2117 IR Spectroscopic Imaging of Heart Transplant Biopsies Towards Improving Detection of Antibody Mediated Rejection

Michael Walsh, Peter Nguyen, Aliya Husain, M Kamran Mirza. University of Illinois, Chicago, IL; University of Chicago, Chicago, IL.

Background: Cardiac transplantation is the preferred treatment for end-stage heart disease and multiple heart biopsies are performed to monitor acute rejection. Histologically, cardiac rejection is categorized into acute cellular and antibody-mediated rejection (AMR). AMR occurs in approximately 10% to 20% of heart transplant patients, and is associated with worse survival, but it is only tested for if there are histologic findings suggesting that AMR is present. Currently, diagnosis of AMR is through

immunofluorescence or immunohistochemical staining, using antibodies for C4d and/or C3d which are complement fragments, within the endothelial layer. Infrared (IR) imaging derives chemical information from inherent biochemistry, giving a measure of levels of biomolecular components (DNA, RNA, carbohydrates, proteins, etc). IR imaging can help classify disease states. In this study, we use IR imaging to find a fingerprint of AMR, and correlate it with immunohistochemical staining for C4d.
Design: Three study groups were created: native heart biopsies (from heart failure patients), transplanted hearts with positive AMR, and transplanted hearts with negative AMR by C4d staining. Each group had five biopsies. Multiple sections were cut: Hematoxylin and Eosin, C4d, CD31, and one unstained for IR imaging. Fourier Transform Infrared (FT-IR) and Quantum Cascade Laser (QCL) were used for IR imaging. Using the multiple stains, regions of interests (ROI) were selected on the IR image: myocardial and endothelial cells. Multivariate analysis and a classifier were used to see how the three groups compared.
Results: Principal component analysis (PCA), a multivariate analysis, was used to find the inter-sample variance across samples and showed grouping within each group. Linear discriminate analysis (LDA), a classifier, was able to separate patients into their respective groups. We were able to find that there was a biochemical difference of AMR positive compared to the other two groups. Myocardial ROIs had a better separation than endothelial ROIs.
Conclusions: In this study, we demonstrated that AMR positive biopsies had a unique fingerprint different from AMR negative and native hearts. Myocardial cells had better separation than endothelial cells, which may indicate AMR affects the whole heart instead of just endothelial cells. IR imaging is a novel tool in the clinical setting of pathology and has the potential to fit into current clinical workflow.

2118 Clinical Experiences of a Custom 68-Gene NGS Panel for Molecular Testing in Solid Tumors

Danbin Xu, Hye Son Yi, Shruti Bhide, Christopher Lunter, Andre Rivera, Anna Berry. CellNetix Pathology & Laboratories, Seattle, WA; Symbiodx, Seattle, WA.
Background: Next-Generation-Sequencing (NGS) enables efficient and cost-effective analysis of a number of cancer-related genes simultaneously to facilitate the clinical decision in cancer diagnosis, prognosis, and treatment management. A 68-gene panel with over 600 amplicons covering more than 4000 potential variants have been developed and validated in our laboratory. Application of this NGS panel complimentary to the anatomic pathology service demonstrates clear clinical benefits for cancer patients.
Design: A standard operating procedure was established through our extensive in-house validation process by using 69 DNA samples extracted from 58 FFPE tissue blocks and 11 whole blood specimen. FFPE tissue sections were reviewed by an onsite pathologist and manually micro-dissected to determine/improve the tumor load. Genomic DNA was used for amplification of targeted regions (Illumina TruSeq Custom Amplicon) and subsequent sequencing analysis on MiSeq using V3-600 chemistry. The raw VCF data is independently analyzed for the presence of any essential actionable mutations, read-depth of the targeted regions, and specimen-specific variants through an in-house developed filtering algorithm. A streamlined bioinformatics pipeline was established and was implemented into the data analysis of clinical specimen.
Results: A total of 216 solid tumor specimens have been tested for this 68-gene panel in the past few months. Lung, colorectal, and breast adenocarcinomas represented the majority of the tumor types being tested which account for 19%, 12.5% and 12% respectively. The average read depth for the target regions is approximately 2,000X to 2,500X and the limit of detection of this assay is at approximately 5% to 10% of the minor allele against the major allele background based on the overall tumor loads of the specimens. Over 800 aberrations have been reported out for the specimen being tested and approximately half of these variants have been reported in the literature. TP53, KRAS, APC and PIK3CA are among the most frequently mutated genes in the specimen tested. Both clinical actionable mutations and clinical applicable mutations have been identified in the same tumor specimen in multiple cases.
Conclusions: Our comprehensive 68-gene NGS panel is a sensitive and specific assay for the hotspot mutations analysis. It provides a highly efficient approach to clinical laboratory for routine molecular oncology testing and additional therapeutic options to cancer patients.

2119 ALK Immunocytochemistry on Cell-Transferred Cytologic Smears of Lung Adenocarcinoma

Chen Zhang, Melissa Randolph, Kelly Jones, Harvey Cramer, Liang Cheng, Howard Wu. Indiana University School of Medicine, Indianapolis, IN.
Background: Anaplastic lymphoma kinase (*ALK*) gene rearrangement defines a subgroup of lung adenocarcinoma that may be successfully treated with the ALK inhibitor crizotinib. ALK immunohistochemical staining (IHC) performed on formalin fixed paraffin embedded tissue or cell blocks (CB) has been reported as an effective and affordable alternative to fluorescence hybridization in situ (FISH) for the detection of *ALK* gene rearrangement. However, cytology smears frequently constitute the only available source of tumor cells due to insufficient CB cellularity. This study is aimed to assess the utility of ALK immunocytochemical staining (ICC) on direct smears using the cell transfer (CT) technique for the detection of *ALK* rearrangement.
Design: Fine needle aspiration (FNA) cases diagnosed as primary or metastatic lung adenocarcinoma in which the status of *ALK* rearrangement had been determined by FISH performed either on CB or concurrent surgical biopsies were identified over a period of 24 months. ICC staining for ALK (clone D5F3) was performed on alcohol-fixed Papanicolaou-stained direct smears using the CT technique. ALK immunoreactivity was evaluated in a modified semiquantitative graded criteria as: score 3+ for strong, granular cytoplasmic staining in most of tumor cells; score 2+ for moderate, smooth cytoplasmic staining in most of tumor cells; score 1+ for faint, focal cytoplasmic staining; and score 0 for complete absence of staining. Scores 2+ and 3+ were reported as positive and scores 1+ and 0 were reported as negative. These ICC results were compared with the corresponding FISH data from the same patients.
Results: A total of 42 FNA specimens from 42 patients were included in this study. 36 were negative and 6 were positive for *ALK* rearrangement on FISH. Four of 6 FISH positive cases showed positive ALK ICC staining (66.7%) and 35 of 36 FISH negative cases were negative on ALK ICC staining (97.2%). The overall correlation between ALK ICC and FISH was 92.9%. The two ICC-/FISH+ cases had low cellularity on direct smears which may account for the false negative results by ICC. The one ICC+/FISH- case had an ICC score 3+.
Conclusions: ICC performed on FNA smears using the CT technique is an acceptable alternative method for assessing *ALK* rearrangement, especially when the direct smears are highly cellular and the CB lacks adequate cellularity.

Ultrastructural Pathology

2120 Undifferentiated Embryonal Sarcoma of Liver in Adult: Unique Ultrastructural Features and Immunophenotypes

Andrew Bandy, Haonan Li, Xiaoming You, Yihe Yang, Jie Liao, MS Rao, William Laskin, Guang-Yu Yang. Northwestern University, Chicago, IL.
Background: Undifferentiated embryonal sarcoma (UES) of the liver is a rare malignancy that occurs predominantly in children, with few reports in adults. The tumor is dominantly composed of primitive mesenchymal elements with few differentiating features. Such morphologic undifferentiated features lead diagnostic difficulty, particularly due to lack of definitive immunostaining, which most times require large, expensive immunostaining panels to be performed. We studied a cohort of liver UES in adults, using electron microscopy (EM) and a panel of immunohistochemical stains to determine tumor cell lineage.
Design: Three cases of UES in the liver were obtained from our institutional pathology database, two found in 17-year old females and one found in a 34-year old female. Histological, immunohistochemistical and ultrastructural studies were employed for all cases.
Results: Morphologically, all three tumors showed a pseudocapsule partially separating the normal liver from undifferentiated sarcomatous cells. Two cases displayed densely cellular areas of predominantly spindle cells and myxoid, paucicellular areas with stellate and spindled cells. Rare large tumor cells with prominent hyaline globules were also seen. One case showed similar morphologic features but had prominent anaplastic/bizarre tumor cells with rhabdoid features and hyaline globules. Ultrastructural studies revealed a background of amorphous collagen-poor matrix containing polygonal cells with a high nuclear to cytoplasmic ratio with abundant organelles, but absence of intracytoplasmic filaments, filament-ribosomal complexes or any other differentiating elements. Degenerative lysosomes were identified in occasional bizarre cells. Immunohistochemical phenotyping demonstrated neoplastic cells were positive for vimentin in all three cases and 2 of the three cases showed positive staining for CD56. One case showed positivity for glypican 3 or desmin. The large tumor cells with prominent hyaline globules showed positivity for D-PAS and CD68. All tumor cells were negative for S100, melan A, myogenin, myoD1, muscle actin and smooth muscle actin, c-kit, DOG-1, CD10, CD99, CD34, Bcl-2, HePar-1, cytokeratin Cam5.2 and AE1/AE3, and EMA.
Conclusions: Our results further support the undifferentiated nature of this tumor and origin from primitive mesenchyme. Although large and expensive immunostaining panels are necessary and function to exclude any potential differentiation, electron microscopy appears to be a unique approach for diagnosis and helps to determine differentiation in the tumor for proper classification.

2121 Human Immunodeficiency Virus in Glomerular Epithelial Cells in HIV-Associated Nephropathy

Xin Gu, Kunle Ojemakinde, Guillermo Herrera. Louisiana State University Health Sciences Center, Shreveport, LA.
Background: HIV-associated nephropathy (HIVAN) is an aggressive kidney disease in HIV-1-infected patients. HIVAN is characterized by the collapse of the glomerular tufts, epithelial (podocyte) hypertrophy/hyperplasia and diffuse foot process effacement with concurrent tubular microcystic dilation and tubulointerstitial nephritis. Podocytes injury is believed a major cause for glomerular morphologic changes in HIVAN.
Both human and animal studies have indicated that glomerular podocytes are not permissive to HIV-1 replication, and pathological changes of podocytes are caused by their exposure to HIV proteins rather than direct virus infection. We are not aware of any previous report of HIVAN that described virus infection and replication in the podocytes in human kidney biopsies. In here, we provide an electron microscopic evidence of HIV infection and replication in podocytes in associated with cellular injury in an HIV patient.
Design: Kidney biopsy tissue was prepared for light microscopy, immunofluorescence and electron microscopy following routinely protocol that is applied for medical renal disease.
Results: The biopsy has 24 glomeruli, 10 of them are sclerotic. Collapsing and usual type segmental sclerosis is seen in 8 viable glomeruli. Interstitial inflammation and tubular microcystic dilation are present. The immunofluorescence study is negative for all reactants. Electron microscopy shows diffuse effacement of foot processes, segmental collapse of glomerular tufts associated with podocyte hyperplasia and fragmentation of cytoplasm. Packed viral particle are present in intact (figure A, B, arrows) as well as fragmented podocytes (figure C, D). The shape and size of viral particles are similar to previously described in infected lymphocytes.